Title: Long-term Air Pollution, Noise, and Structural Measures of the Default Mode Network in the Brain: Results from the 1000BRAINS Cohort

Authors: Sarah Lucht[a,1], Lina Glaubitz[a], Susanne Moebus[b], Sara Schramm[c], Christiane Jockwitz[d,e], Svenja Caspers[d,e,f]*, and Barbara Hoffmann[a]*.

a) Environmental Epidemiology Group, Institute of Occupational, Social and Environmental Medicine, Centre for Health and Society, Medical Faculty and University Hospital Düsseldorf, Heinrich Heine University Düsseldorf, Düsseldorf, Germany
b) Institute for Urban Public Health, University Hospital Essen, University of Duisburg-Essen, Essen, Germany
c) Institute of Medical Informatics, Biometry and Epidemiology, University Hospital Essen, University of Duisburg-Essen, Essen, Germany
d) Institute of Neuroscience and Medicine (INM-1), Research Centre Jülich, Jülich, Germany
e) Institute for Anatomy I, Medical Faculty and University Hospital Düsseldorf, Heinrich Heine University Düsseldorf, Düsseldorf, Germany
f) JARA-BRAIN, Jülich-Aachen Research Alliance, 52425 Jülich, Germany

*Contributed equally to this work

1. Corresponding Author: Sarah Lucht, Universitätsklinikum Düsseldorf, AG Umweltepidemiologie, Postfach 101007, 40001 Düsseldorf, Germany. E-mail address: sarah.lucht@uni-duesseldorf.de.

Competing Financial Interests: The authors declare they have no actual or potential competing financial interests.

Abstract

Background: While evidence suggests that long-term air pollution (AP) and noise may adversely affect cognitive function, little is known about whether environmental exposures also promote structural changes in underlying brain networks. We therefore investigated the associations between AP, traffic noise, and structural measures of the Default Mode Network (DMN), a functional brain network known to undergo specific changes with age.

Methods: We analyzed data from 579 participants (mean age at imaging: 66.5 years) of the German 1000BRAINS study. Long-term residential exposure to particulate matter (diameter ≤10 µm [PM_{10}]; diameter ≤2.5 µm [$PM_{2.5}$]), $PM_{2.5}$ absorbance ($PM_{2.5abs}$), nitrogen dioxide (NO_2), and accumulation mode particulate number concentration (PN_{AM}) was estimated using validated land use regression and chemistry transport models. Long-term outdoor traffic noise was modeled at participants' homes based on a European Union's Environmental Noise Directive. As measures of brain structure, cortical thickness and local gyrification index (lGI) values were calculated for DMN regions from T1-weighted structural brain images collected between 2011 and 2015. Associations between environmental exposures and brain structure measures were estimated using linear regression models, adjusting for demographic and lifestyle characteristics.

Results: AP exposures were below European Union standards but above World Health Organization guidelines (e.g., PM_{10} mean: 27.5 µg/m^3). A third of participants experienced outdoor 24-hour noise above European recommendations. Exposures were not consistently associated with lGI values in the DMN. We observed weak inverse associations between AP and cortical thickness in the right anterior DMN (e.g., -0.010 mm [-0.022, 0.002] per 0.3 unit increase in $PM_{2.5abs}$) and lateral part of the posterior DMN.

Conclusion: Long-term AP and noise were not consistently associated with structural parameters of the DMN in the brain. While weak associations were present between AP exposure and cortical thinning of right hemispheric DMN regions, it remains unclear whether AP might influence DMN brain structure in a similar way as aging.

Keywords: Air pollution, particulate matter, brain imaging, brain structure, cognitive function

Abbreviations: AD, Alzheimer's Disease; aDMN, anterior Default Mode Network; AP, air pollution; BMI, body mass index; DAG, directed acyclic graph; dB(A), A-weighted decibels; DMN, Default Mode Network; ESCAPE, European Study of Cohorts for Air Pollution Effects; EURAD, European Air Pollution Dispersion; ETS, environmental tobacco smoke; GMV, gray matter volume; HNR, Heinz Nixdorf Recall; I-L_{den}, indoor 24-hour weighted traffic noise; I-L_{night}, indoor nighttime traffic noise; IQR, interquartile range; iSES, individual socioeconomic status; L_{den}, outdoor 24-hour weighted traffic noise; lGI, local gyrification index; L_{night}, outdoor nighttime traffic noise; LUR, land use regression; MP-RAGE, magnetization-prepared rapid acquisition gradient-echo; MRI, magnetic resonance imaging; NO_2, nitrogen dioxide; nSES, neighborhood socioeconomic status; PASA, posterior-anterior shift in aging; pDMN, posterior Default Mode Network; $M_{2.5}$, particulate matter with aerodynamic diameter ≤ 2.5 μm; $PM_{2.5abs}$, absorbance of particulate matter with aerodynamic diameter ≤ 2.5 μm; PM_{10}, particulate matter with aerodynamic diameter ≤ 10 μm; PN_{AM}, accumulation mode particle number concentration; ρ, Spearman correlation coefficient; SD, standard deviation; WMV, white matter volume

1. Introduction

Air pollution (AP), defined as a harmful mixture of gases and particles in the air, is a known risk factor for cardiovascular and respiratory diseases as well as mortality across the world (Schraufnagel et al., 2019; Thurston et al., 2017). Recent experimental and epidemiologic evidence suggests that AP exposure may also adversely affect the brain via systemic inflammation and direct translocation of small particles into the brain (Genc et al., 2012). Epidemiologic studies support that higher AP exposure is linked to decreases in cognitive function (Paul et al., 2019), including in memory function (e.g., Nußbaum et al., 2020; Tonne et al., 2014; Tzivian et al., 2016b).

With growing evidence that AP exposure may accelerate cognitive decline, several observational studies have investigated whether AP exposure is also associated with adult brain structure. Associations between AP exposure and lower brain volume have been observed in multiple studies (e.g., Erickson et al., 2020; Gale et al., 2020), but results are difficult to compare across differing brain regions. In studies all conducted in the UK Biobank cohort utilizing the same AP exposures ($PM_{2.5}$, PM_{10}, NO_x, NO_2, and PM_{coarse}), they observed inverse associations between $PM_{2.5}$, PM_{10}, NO_x and prefrontal volume (Gale et al., 2020), PM_{coarse} and volume in the left thalamus (Hedges et al., 2020), and $PM_{2.5}$ and left hippocampal volume (Hedges et al., 2019). Non-volumetric measures of brain structure, such as region-specific cortical thickness, have been studied less frequently than volumetric measures. Results from two cortical thickness studies suggest that AP may be associated with reduced cortical thickness in some areas (e.g., frontal and temporal cortices [Cho et al., 2020]; Alzheimer's associated areas [Crous-Bou et al., 2020]) but increased thickness in others (e.g., occipital and cingulate cortices [Cho et al., 2020])

Alongside AP, chronic noise exposure has emerged as an important environmental factor and co-exposure (e.g., through traffic) that also exerts adverse effects on human health. Long-term noise exposure has been linked to increased risk of non-auditory outcomes (e.g., cardiovascular disease, depression), with potential mechanisms including increased stress due to sleep disturbances and increased annoyance (Basner et al., 2014). Noise has also been linked to decreases in cognitive function, including poorer memory among children (Basner et al., 2014), increased risk of mild cognitive impairment (Tzivian et al., 2016b), and decreased memory function among adults (Tzivian et al., 2016a; Wright et al., 2014). At present, only three studies have examined how chronic noise exposure may influence adult brain structure with one showing

adverse effects on gray matter volume (Cheng et al., 2019), one showing no effect on cortical thickness and regional volumes (Crous-Bou et al., 2020), and one showing null and positive associations with gyrification, a measure of brain folding (Nußbaum et al., 2020).

While the study of long-term AP, noise, and brain health is relatively new, research supports that normal aging is consistently accompanied by global and region-specific changes in both brain function and structure. Structurally, old age is associated with decreased global cortical surface area as well as region-specific brain volume and cortical thickness, changes which have been linked to decreases in cognitive function (Gautam et al., 2015; Jockwitz et al., 2019; Tsapanou et al., 2019). Local Gyrification Index (lGI), a measure of local surface structure that is thought to be rather sensitive, is also known to decrease with age (Hogstrom et al., 2013). Likewise, age-related changes in functional brain networks, which are regions that show highly correlated activity levels, have also been identified using imaging studies (e.g., Davis et al., 2008; Jockwitz et al., 2017). To date, Nußbaum et al. (2020)'s work in the fronto-parietal network is the only study to have looked at AP and brain structure in a functionally important brain network. They observed that AP exposures were inversely associated with lGI in the right hemisphere of the fronto-parietal network, results which are consistent with effects observed during aging. In conjunction with studies showing decreased cognitive function with higher AP exposure (Paul et al., 2019), this suggests that AP may accelerate or mimic the processes in the brain that occur with aging. Nevertheless, more work is needed before such conclusions can be made.

Composed of three bilateral regions in the brain, the Default Mode Network (DMN) is an important functional network that plays a large role in mental functions, such as self-referential thinking, and memory recall (Raichle, 2015). While the DMN is generally deactivated during externally-focused, attention-demanding activities, it is activated during the resting state (Raichle, 2015). Aging of this network is associated with changes in functional connectivity, including a posterior to anterior shift (PASA) where frontal brain regions take over additional functions to compensate for decreased activity in posterior regions (Davis et al., 2008). These changes in functional connectivity are reflected in structural changes locally, with greater relative decreases in lGI observable in posterior brain regions of the DMN than in the anterior regions (Jockwitz et al., 2019; Jockwitz et al., 2017). Jockwitz et al. (2017) also observed larger age-associated structural differences in the right hemisphere of the DMN, consistent with the right hemi-aging theory that the right hemisphere is more susceptible to the effects of aging than the left (Brown and Jaffe, 1975; Dolcos et al., 2002). Nußbaum et al. (2020) also observed that AP was more

strongly associated with lower lGI in the right hemisphere of the fronto-parietal network compared to the left.

Despite the DMN's role in memory recall and previous studies linking AP and noise exposures to changes in memory-related brain functions, no studies have investigated how AP and noise exposures may influence brain structure in the DMN and whether these environmental exposures exert similar effects as observed with aging. We therefore investigated the associations between long-term ambient exposure to AP, road traffic noise, and structural measures of the DMN (cortical thickness, lGI) in the German 1000BRAINS study in order to evaluate the role these environmental exposures may have on brain structure. We hypothesized that higher exposure to AP and noise would be associated with decreased cortical thickness and lGI in the regions of the DMN, similar to what would be expected with aging.

2. Methods

2.1 Study population

This study was conducted using data from the 1000BRAINS Study, an epidemiologic population-based study designed to investigate the variability of brain structure, function, and connectivity during the normal aging process (Caspers et al., 2014). Participants of the 1000BRAINS study were recruited from the prospective Heinz Nixdorf Recall (HNR) study and the HNR MultiGeneration Study in the highly urbanized German Ruhr area (Essen, Bochum, Mülheim), but the current study includes only HNR participants of the 1000BRAINS participants, as no environmental exposure data is currently available for the HNR MultiGeneration Study. The HNR study has been described in detail previously (Schmermund et al., 2002; Stang et al., 2005). Briefly, middle- to older-aged participants (45-74 years) were randomly selected from city residential registries and recruited via mail (recruitment efficiency proportion: 55.8%; Stang et al., 2005). Participants completed baseline (2000-2003; n=4,814), 5-year follow-up (2006-2008; n=4,157), and 10-year follow-up (2011-2015; n=3,087) examinations. At each examination, extensive sociodemographic, lifestyle, morbidity, and laboratory information was collected. HNR participants were approached about 1000BRAINS participation at the 10-year follow-up examination, with the requirement that they were willing to travel the 100-120 km distance to the MRI study and did not have debilitating diseases (Caspers et al., 2014). Subjects were also excluded from participation in the 1000BRAINS study if they

were not eligible for having magnetic resonance imaging (MRI) measurements taken (i.e., claustrophobia, history of neurosurgery, presence of tattoos or permanent makeup on the head, cardiac pacemakers, surgical implants or prostheses in the trunk or head, coronary artery stents, and potentially dental implants and bridges producing artifacts in the images). Eligible and willing participants (n=688) underwent MRI scans as well as neuropsychological and motor assessments between 2011 and 2015 (Fig. 1; more details in Caspers et al., 2014 and section 2.4). Any participants whose MRI showed conditions requiring immediate medical protocol (e.g., acute stroke, aneurysm) or medical referral (e.g., post-stroke status) were excluded from the study, but normal aging-associated brain changes were not considered criteria for exclusion. Protocols for both the HNR and 1000BRAINS studies were approved by the local Ethics Committee of the University of Essen. All participants gave written informed consent.

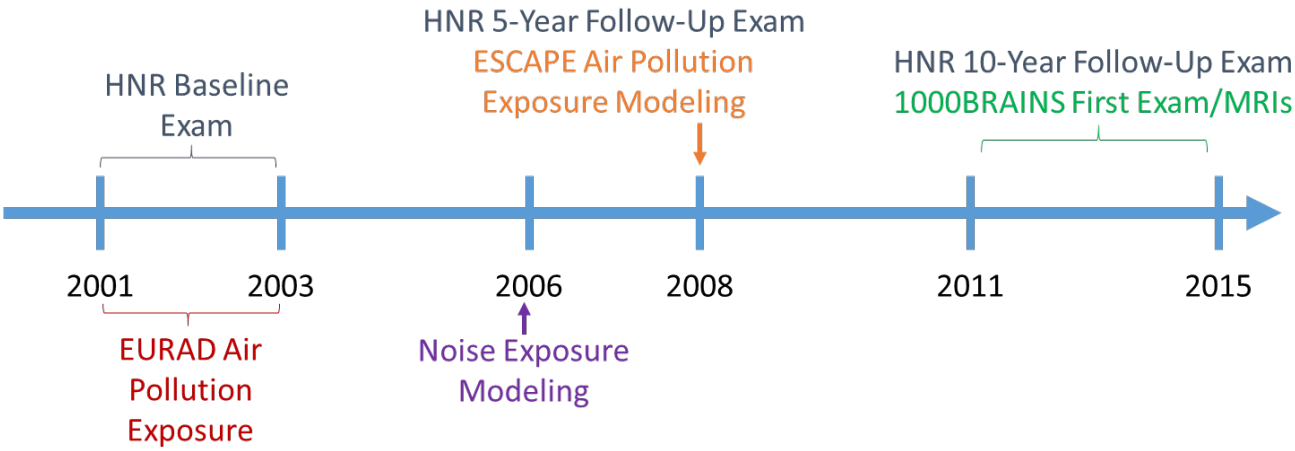

Fig. 1. Timeline showing when health examinations for the HNR as well as 1000BRAINS studies took place as well as when the air pollution and noise exposures were assessed. The ESCAPE and noise modeling estimates, while taking place later, were assigned to the residential addresses for HNR participants at baseline (2001-2003). *Abbreviations:* ESCAPE, European Study of Cohorts for Air Pollution Effects; EURAD, European Air Pollution Dispersion; HNR, Heinz Nixdorf Recall; MRI, magnetic resonance imaging

2.2 Air Pollution Exposures

Two air quality models were utilized for estimating long-term exposures in this study. Long-term exposure to particulate matter with aerodynamic diameter ≤ 2.5 µm ($PM_{2.5}$; µg/m^3), particulate matter with aerodynamic diameter ≤ 10 µm (PM_{10}; µg/m^3), $PM_{2.5}$ absorbance ($PM_{2.5abs}$; 0.0001/m), and nitrogen dioxide (NO_2; µg/m^3) was estimated using the European Study of Cohorts for Air Pollution Effects (ESCAPE) land use regression (LUR) model. This LUR model uses land use data to predict temporally-stable, point-specific AP exposures and was

built following the standards of the European-wide ESCAPE project (more details provided in Cyrys et al., 2012; Eeftens et al., 2012). Briefly, the ESCAPE project was designed to investigate the effect of long-term air pollution on health using prospective cohort studies in 15 countries across Europe. LUR prediction models were built within each study according to common guidelines (Eeftens et al., 2012) using data from individual measurement campaigns and local geographic data (e.g., traffic density, population density). For the Ruhr area, PM (20 sites) and NO_2 (40 sites) data were collected between October 2008 and October 2009 (Hennig et al., 2016). Detailed information on the geographic data included in the specific AP models can be found in Eeftens et al., (2012) and Beelen et al., (2013). The ESCAPE models explained a large proportion of the variance in annual AP concentrations in the Ruhr area (69% for PM_{10}, 88% for $PM_{2.5}$, 97% for $PM_{2.5abs}$, and 89% for NO_2; Eeftens et al., 2012). Each participant of the HNR was assigned point-specific exposure estimates for their residence at the baseline examination (2001-2003). Residence at baseline was chosen for exposure estimation (approximately 10 years prior to MRI), because mechanistic hypotheses suggest that environmental effects on the brain likely accumulate over an extended period of time (Block and Calderón-Garcidueñas, 2009).

Particle number concentrations (PN_{AM}; n/mL) for the accumulation mode (mean diameter: 0.07 µm; 67% of particles with aerodynamic diameters between 0.035 and 0.14 µm) were estimated for all participants using the validated, time-dependent, three-dimensional EURopean Air pollution Dispersion (EURAD) chemistry transport model (Memmesheimer et al., 2004; Nonnemacher et al., 2014). Using multiple layers and grids, the EURAD model simulates the chemical transformation, deposition, and transport of AP on both local and regional levels (Memmesheimer et al., 2004). It uses four sequential nesting grids (125 km, 25 km, 5 km, and 1 km) to estimate hourly exposures for Europe, central Europe, the state of North Rhine-Westphalia in northwestern Germany, and the Ruhr Area, respectively. PN_{AM} exposure estimates have been validated against measurements taken using a TSI 3926 scanning mobility particle size spectrometer (size range: 0.014-0.750 µm; TSI Inc., Shoreview, MN, USA) at the Mülheim-Styrum monitoring station for the period 2011-2014 (Birmili et al., 2016). Pearson correlations were moderate (r=0.57) for daily measurements, with strongest seasonal correlations seen during winter and fall (r=0.61; Lucht et al., 2019). According to the 1 km^2 grid in which their residence was located, HNR participants were assigned mean PN_{AM} values for the baseline HNR period (2001-2003; ArcView, version 9.2, ESRI, Redlands, CA, USA).

2.3 Long-Term Traffic Noise Exposure

As required by the European Union Directive 2002/49/EC (European Environment Agency, 2002), long-term road traffic noise was modeled for the year 2006 on behalf of local city administrations, who supplied source-specific noise values from the VBUS/RLS-90 method (Bundesministerium der Justiz, 2006) using CadnaA software (DataKustik GmbH.). Outdoor weighted 24-hour noise (L_{den}; A-weighted decibels [dB(A)]) as well as outdoor nighttime noise (between 22:00 and 6:00; L_{night}) were modeled at façade points (height of 4 m ± 0.2 m) using small-scale topography, building dimensions, speed limit, street axis, noise barriers, type-specific vehicle traffic density, and road surface (Bundesministerium der Justiz, 2006). For L_{den}, daytime noise (6:00-18:00), evening noise (18:00-22:00), and nighttime noise (22:00-6:00) were weighted differently, under the assumption that excess noise in the evening and at night is more disturbing than daytime noise (WHO Regional Office for Europe, 2009). As such, penalties of 5 dB(A) and 10 dB(A) were added to evening and nighttime noise levels, respectively. Outdoor exposures were assigned to participants using the maximum estimated noise value in a 10-m buffer around each participant's address at baseline HNR examination. In analyses, outdoor L_{den} and L_{night} were modeled as a truncated continuous variables with lower thresholds of 45 dB(A) and 35 dB(A), respectively (Ohlwein et al., 2019). Participants were assigned noise values according to their baseline addresses.

Along with outdoor façade noise, we estimated indoor 24-hour and nighttime noise levels using self-reported behavioral and apartment information based on a method by Foraster et al. (2014). It is described in detail for the HNR cohort in Ohlwein et al. (2019). Briefly, indoor L_{den} (I- L_{den}) was estimated in participants' living rooms whereas indoor L_{night} (I- L_{night}) estimates reflect bedroom levels. These estimates were derived from outdoor estimates, with various factors resulting in reduction of noise. If the room was orientated towards a direction other than the postal address street, 20 dB(A) were deducted. When persons reported usually having their windows closed, we subtracted 30 dB(A) if they had single-glazed windows and 40 dB(A) if they had double-glazed windows. For persons who often, seldom, and never closed their windows, we deducted 21 dB(A), 16 dB(A), and 15 dB(A) from outdoor levels, respectively, as described in Ohlwein et al. (2019). I-L_{den} and I-L_{night} were modeled with lower threshold values of 20 dB(A) and 10 dB(A), respectively, in the analyses.

2.4 Brain Structure Measures in Regions of the DMN

Brain images were acquired for all participants included in 1000BRAINS using Magnetic Resonance Imaging on a 3T Siemens Tim-TRIO MR scanner (Erlangen, Germany), using a 32-channel head coil (Caspers et al. [2014]). In order to examine brain structure, i.e., cortical thickness and lGI, a 3D high-resolution T1-weighted magnetization-prepared rapid acquisition gradient-echo (MP-RAGE) anatomical scan was acquired and used for subsequent surface reconstruction (176 slices, slice thickness: 1 mm, repetition time: 2250 ms, echo time: 3.03 ms, field of view: 256 x 256 mm^2, flip angle: 9°, voxel resolution: 1 mm^3).

The identification of the DMN was part of a previous study and has been described elsewhere in detail (Jockwitz et al., 2017). Briefly, 691 resting-state scans were preprocessed using the FMRIB Software Library processing pipeline (http://www.fmrib.ox.ac.uk/fsl; Jenkinson et al., 2012). Afterwards, common spatial patterns across subjects within the resting state data were identified using MELODIC (Beckmann et al., 2005). For reliability purposes, this procedure was repeated 100 times, with each sample consisting of 200 randomly selected subjects. For each group, the DMN was selected and all DMNs were superimposed onto each other resulting in a probability map, which was thresholded at 95% (using fslmaths, FSL) and binarized. Finally, the DMN was composed of six clusters: two anterior (left and right prefrontal cortex) and four posterior (left and right posterior cingulate cortex/precuneus; left and right angular gyrus; Jockwitz et al., 2017). In analyses, the prefrontal cortex region was denoted as the anterior DMN (aDMN) while the posterior parts were denoted as the medial (cingulate cortex/precuneus) and lateral (angular gyrus) pDMN (Fig. 2).

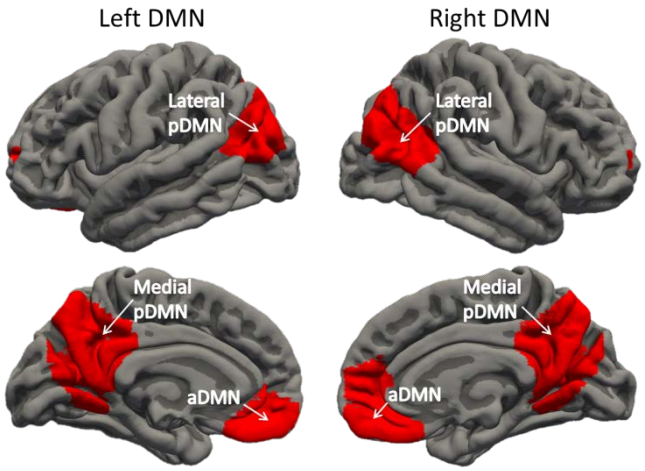

Fig. 2. The Default Mode Network (DMN) projected on the right and left hemispheres of a brain consisting of the lateral posterior DMN (pDMN), medial pDMN, and anterior DMN (aDMN).

In order to calculate cortical thickness and local gyrification indices within all parts of the DMN (Jockwitz et al., 2019; Jockwitz et al., 2017), anatomical images were preprocessed using the automated surface-based processing stream implemented in FreeSurfer (version 6.0.0; for a detailed description of the surface reconstruction, see Dale et al., 1999; Fischl et al., 1999). Based on the reconstructed surfaces, LGI values were calculated according to Schaer et al. (2012) for each part of the DMN as the ratio between the total pial surface area (including sulci) to the outer hull surface area (excluding sulci). Mean cortical thickness (CT; for a detailed overview, see Fischl and Dale, (2000)) was calculated for each DMN region as the shortest distance (mm) between a vertex on the white matter surface and the corresponding vertex on the pial surface.

2.5 Definition of Covariates

Variables from the baseline HNR examination were used in all analyses, with the exception of age (years), where age at time of 1000BRAINS examination was used. Smoking status was defined as current, former (>1 year since quitting), or never smoker. Cumulative smoking exposure (pack-years) was assessed for former and current smokers and accounted for periods of non-smoking. Exposure to environmental tobacco smoke (ETS; Yes/No) was defined as regular passive exposure to smoke at home, work, or other location. Physical activity (Yes/No) was assessed as regular sporting activities at least once a week for a minimum of 30 minutes. Alcohol consumption was obtained through dietary questionnaire and divided into five categories (0, 1-3, 4-6, 6-14, and >14 drinks per week). Anthropometric measurements (height, weight) were measured at examinations according to standard protocols, and body mass index (BMI) was calculated as kilograms per meter squared. Quality of diet was assessed using a dietary pattern index, created by incorporating consumption frequency of 13 food items and diet quality classifications used in previous studies (Winkler and Döring, 1998, 1995). Possible scores ranged from 0-26 with 26 representing an ideal diet and were categorized into three categories (Unfavorable Diet, Normal Diet, Favorable Diet). Individual socioeconomic status (iSES) was defined as years of education, as classified by the International Standard Classification of Education (UNESCO, 1997), and divided into four categories (≤10, 11-13, 14-17, ≥18 years). For neighborhood SES (nSES), unemployment rates (units of percent) between 2001-2003 were obtained from local census authorities for each residential neighborhood according to administrative boundaries (median size: 11,263 inhabitants; Dragano et al., 2009). Nearness of a

participant's residence to a major road (Yes/No), defined as ≤50 m from a main road or ≤100 m from a motorway, was calculated using official digitized maps with a precision of at least 0.5 m.

2.6 Statistical Analysis

We investigated the association between long-term ambient AP and road traffic noise exposures and structural brain parameters (lGI; cortical thickness) in the DMN using linear regression models. Individual models were conducted for the aDMN, medial pDMN, lateral pDMN on both the right and left hemispheres. The normality of residuals was confirmed for the models using Q-Q plots, and the appropriateness of restricted cubic spline terms (knots=4) for continuous variables was assessed in exposure-free models. Associations were estimated as the absolute difference in the outcome per interquartile (IQR) increase for air pollutants or per 10 dB(A) increase for noise exposures and presented alongside 95% confidence intervals.

Three models of increasing covariate adjustment were conducted. Model 1 included the AP or noise exposure, age at MRI and sex. In addition to age and sex, variables in Model 2 were identified using a directed acyclic graph (DAG; Fig. S1) and included alcohol consumption, BMI, diet, physical activity, and smoking (status; cumulative; ETS). The DAG was built using DAGitty software, which outputs minimal sufficient adjustment sets, (Textor et al., 2011) and included variables selected based on prior literature. For the Main Model (Model 3), all AP models were additionally adjusted for outdoor L_{den} whereas noise models were additionally adjusted for $PM_{2.5abs}$. Model 3 also included adjustment for all Model 2 variables.

Multipollutant models were conducted in order to investigate independence of effects by the various exposures. PM models were adjusted separately for NO_2 and PN_{AM}, NO_2 models were adjusted separately for $PM_{2.5}$ and PN_{AM}, and PN_{AM} models were adjusted separately for NO_2 and $PM_{2.5}$. In order to compare effect sizes between age and environmental exposures, we also conducted a secondary analysis examining the association between age and brain structure measures for DMN regions. Age models were adjusted for Main Model variables, with the addition of iSES and nSES, and associations were estimated per one-year increase in age at MRI. As indoor noise values were missing for approximately 10% of the analysis group (n=61), we also conducted a secondary analysis for outdoor and indoor noise within this smaller group (n=518) and using the Main Model adjustment set.

2.7 Effect Modification & Sensitivity Analyses

We evaluated potential effect modification by age at MRI using the addition of an interaction term between the AP exposure and a binary categorization of age (<65 years vs. 65+ years). Several sensitivity analyses were also conducted to assess the robustness of our results. To assess sensitivity to socioeconomic variables, we conducted models including all Main Model variables plus iSES and nSES. As updated information on several HNR baseline lifestyle factors was also collected at the 1000BRAINS recruitment, we also conducted a model utilizing the updated data from the later examination. We restricted our population to participants who reported working less than 15 hours per week, as we expected these participants to spend a greater proportion of their time at home and therefore errors in exposure estimates may be smaller. Additionally, we evaluated the associations using residential address at the 5-year follow-up HNR examination (2006-2008) and among participants who still resided at their baseline addresses at the 10-year follow-up examination (n=442). As several previous studies have looked at residential distance to major roads as a proxy for traffic exposure (Kulick et al., 2017; Nußbaum et al., 2020; Wilker et al., 2016; Wilker et al., 2015), we also evaluated this exposure (residence ≤ 50 m from a federal or main road or ≤ 100 m from a motorway) in a sensitivity analysis. Because some participants were excluded due to missing information, we compared those excluded with the participants included in the analysis as well as with all participants who attended the 10-year follow-up HNR examination.

3. Results

3.1 Study Population

Overall, 688 participants of the 1000BRAINS study were recruited from the HNR study. Of these, participants were excluded from the analysis due to missing brain structure measures (n=85), AP exposures (n=5), outdoor noise levels (n=2), or adjustment variables (n=17; Fig. S2). The final study population therefore included 579 participants. In general, the study population was in late middle age at HNR baseline (mean age: 56.2 years [SD: 6.7], range: 45-74 years), approximately 10 years older at time of MRI (mean age: 66.5 years [SD 6.7], range: 56-85 years), slightly overweight (mean BMI: 27.3 kg/m^2 [SD: 4.1]), and had slightly more men than women (54.2% Male; Table 1). Most participants had at least 11 years of education and did not currently smoke. For observed time-varying lifestyle factors, participants had similar values at baseline and 1000BRAINS recruitment, with the exception of a shift from current smoking to former smoking

and greater exposure to environmental tobacco smoke at the later time point (Table 1). Participants excluded from the analysis were very similar to those included (Table S1), with excluded participants slightly more likely to be male. On average, HNR participants who also took part in the 1000BRAINS study were slightly younger, more male, more likely to eat an unhealthy diet and drink more, and more highly educated than the average participant at the 10-year follow-up HNR examination (Table S1).

Table 1. Demographic and lifestyle characteristics of the 1000BRAINS study participants (n=579) at HNR baseline (2000-2003) and, when updated information was collected[a], at recruitment for 1000BRAINS (2011-2015).

	HNR Baseline	**1000BRAINS Recruitment**
Variable	Mean ± SD or Median [IQR] or n (%)	Mean ± SD or Median [IQR] or n (%)
Age (years)	56.2 ± 6.7	66.5 ± 6.7
BMI (kg/m^2)	27.3 ± 4.1	28.3 ± 4.4
Neighborhood Unemployment (%)	12.1 ± 3.3	-
Female	265 (45.8)	265 (45.8)
Formal Education		
≤10 years	32 (5.5)	32 (5.5)
11-13 years	302 (52.2)	302 (52.2)
14-17 years	143 (24.7)	143 (24.7)
≥18 years	102 (17.6)	102 (17.6)
Physical Activity, Yes	362 (62.5)	373 (64.5)
Smoking Status		
Never Smoker	250 (43.2)	250 (43.3)
Former Smoker	214 (37.0)	263 (45.5)
Current Smoker	115 (19.9)	65 (11.2)
Cumulative Smoking (pack-years)	18.8 [25.0]	-
Environmental Tobacco Smoke Exposure, Yes	225 (38.9)	380 (66.0)
Alcohol Consumption (Drinks/Week)		
Never	226 (39.0)	-
1 to 3	96 (16.6)	-
>3 to 6	80 (13.8)	-
>6 to 14	87 (15.0)	-
>14	90 (15.5)	-
Diet		
Unfavorable Diet	235 (40.6)	235 (40.9)
Normal Diet	209 (36.1)	192 (33.4)
Favorable Diet	135 (23.3)	147 (25.6)

Abbreviations: BMI, body mass index; HNR, Heinz Nixdorf Recall; IQR, interquartile range; MRI, magnetic resonance imaging; SD, standard deviation

[a]Data available only at baseline examination for neighborhood unemployment, cumulative smoking, and alcohol consumption

Air pollution levels at participants' homes were below the European Union Air Quality Standards for annual concentrations (40 µg/m^3 for NO_2 and PM_{10}, 25 µg/m^3 for $PM_{2.5}$; Table 2;

European Parliament, Council of the European Union, 2008), but above the World Health Organization's Air Quality Guidelines for annual PM_{10} and $PM_{2.5}$ (20 μg/m^3 and 10 μg/m^3, respectively; World Health Organization [2006]). Mean 24-hour outdoor noise levels were slightly below the European L_{den} guideline of 53 dB(A), with 203 participants (35.1%) exposed to noise levels above this recommendation (World Health Organization, 2018). AP exposures were moderately to highly correlated with each other (Spearman correlations [ρ]: 0.49-0.91) and weakly correlated with noise exposures (ρ: 0.08-0.41; Table S2). Outdoor L_{den} and L_{night} were highly correlated (ρ: 0.99), whereas outdoor and indoor noise exposures were only moderately correlated (ρ: 0.40-0.50; Table S2). LGI values were, on average, higher in the posterior regions of the DMN than in the anterior DMN, whereas cortical thickness was slightly lower in the medial pDMN compared to other regions (Table S3).

Table 2. Description of long-term air pollution and noise exposure levels at the baseline residential addresses of 1000BRAINS study participants.

Exposure	Mean ± SD or n (%)	Interquartile Range
Air Pollution		
PM_{10} (μg/m^3)	27.5 ± 1.8	2.1
$PM_{2.5}$ (μg/m^3)	18.2 ± 1.0	1.4
$PM_{2.5abs}$ (0.0001/m)	1.5 ± 0.4	0.3
NO_2 (μg/m^3)	29.5 ± 4.6	5.2
PN_{AM} (n/mL)	3,725 ± 435	612
Near Major Road (Yes)	109 (18.8)	-
Noise		
Outdoor L_{den} (dB[A])	53.4 ± 8.4	13.1
Outdoor L_{night} (dB[A])	44.4 ± 8.3	12.7
Indoor L_{den} (dB[A])	35.1 ± 12.5	20.6
Indoor L_{night} (dB[A])	27.3 ± 13.8	24.1

Abbreviations: dB(A), A-weighted decibels; L_{den}, outdoor 24-hour weighted noise; L_{night}, outdoor nighttime noise; NO_2, nitrogen dioxide; PM_{10}, particulate matter with diameter ≤10 μm; $PM_{2.5}$, particulate matter with diameter ≤2.5 μm; $PM_{2.5abs}$, $PM_{2.5}$ absorbance; PN_{AM}, accumulation mode particle number concentration; SD, standard deviation

3.2 Model Adjustment & Main Results

Only results from the Main Model (Model 3) will be presented in detail here, as increasing adjustment for potential confounders did not result in large changes in the estimated associations between AP, noise, and brain structure measures (Fig. S3). Interestingly, adjustment for co-exposures (i.e., L_{den} for AP exposures and $PM_{2.5abs}$ for noise exposures) did not result in qualitative changes in the estimated associations.

For lGI, no consistent associations were observable with AP and noise exposures across the various regions and two hemispheres (Fig. 3; AP estimates in Table S4). Point estimates for AP exposures were all associated with slightly lower lGI in the left aDMN, whereas several AP exposures were associated with slightly higher lGI in the lateral pDMN and medial pDMN. Results for outdoor noise exposures were similarly mixed (Fig. 3). Age at MRI was inversely associated with lGI in the lateral pDMN regions (Fig. 3).

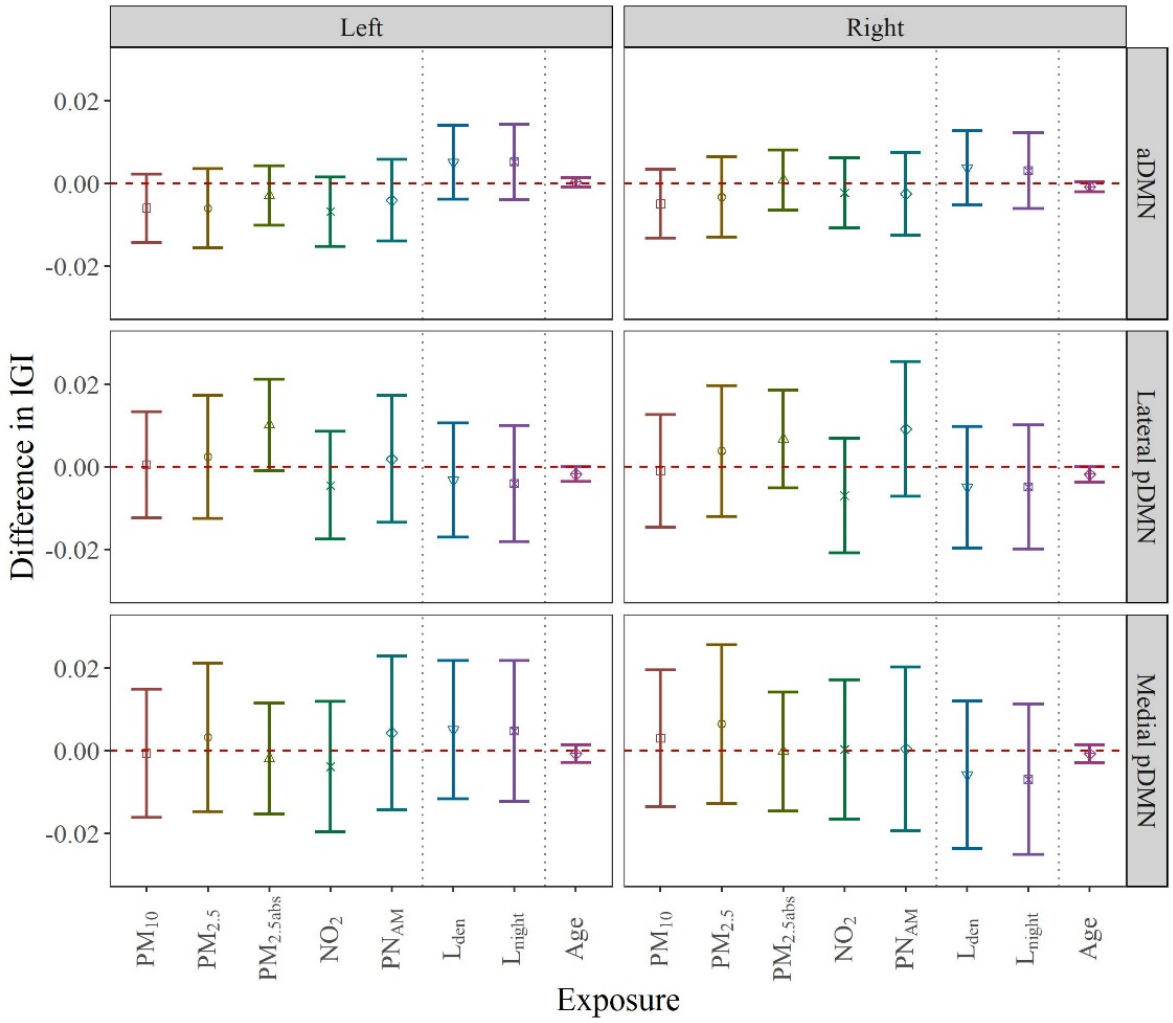

Figure 3. Associations between AP, noise, and lGI within regions of the DMN in the right and left hemispheres of the brain. AP and noise estimates were calculated per IQR increase and per 10 dB(A), respectively, and are shown with 95% confidence intervals. Models were adjusted for age at MRI, sex, alcohol consumption, body mass index, diet, physical activity, smoking status, cumulative smoking, and environmental tobacco smoke exposure. AP models were additionally adjusted for 24-hour outdoor noise and noise models were adjusted for $PM_{2.5abs}$. For reference, age at MRI and lGI was also modeled per 1-year increase and adjusting for sociodemographic variables included in the AP models as well as iSES and nSES.

Abbreviations: aDMN, anterior Default Mode Network; AP, air pollution; DMN, Default Mode Network; pDMN, posterior Default Mode Network; iSES, individual socioeconomic status; L_{den}, outdoor 24-hour weighted noise; lGI, local gyrification index; L_{night}, outdoor nighttime noise; MRI, magnetic resonance imaging; NO_2, nitrogen dioxide;

nSES, neighborhood socioeconomic status; PM_{10}, particulate matter with diameter ≤10 μm; $PM_{2.5}$, particulate matter with diameter ≤2.5 μm; $PM_{2.5abs}$, $PM_{2.5}$ absorbance; PN_{AM}, accumulation mode particle number concentration

Higher AP exposure was weakly associated with lower cortical thickness in the right aDMN and lateral pDMN for all air pollutants (Fig. 4; AP estimates in Table S5). In the left aDMN, results were more inconsistent, with some negative and null associations present. In contrast, increases in outdoor 24-hour and nighttime noise exposure were associated with higher cortical thickness in the right aDMN. Age at MRI was inversely associated with cortical thickness in all regions, with strongest associations apparent in the pDMN regions (Fig. 4). In the right aDMN, AP exposures were more inversely associated with cortical thickness (e.g., -0.010 [95% CI: -0.022, 0.002] per IQR increase in $PM_{2.5abs}$) than a 1-year increase in age (-0.001 mm [95% CI: -0.003, 0.001] per 1-year increase).

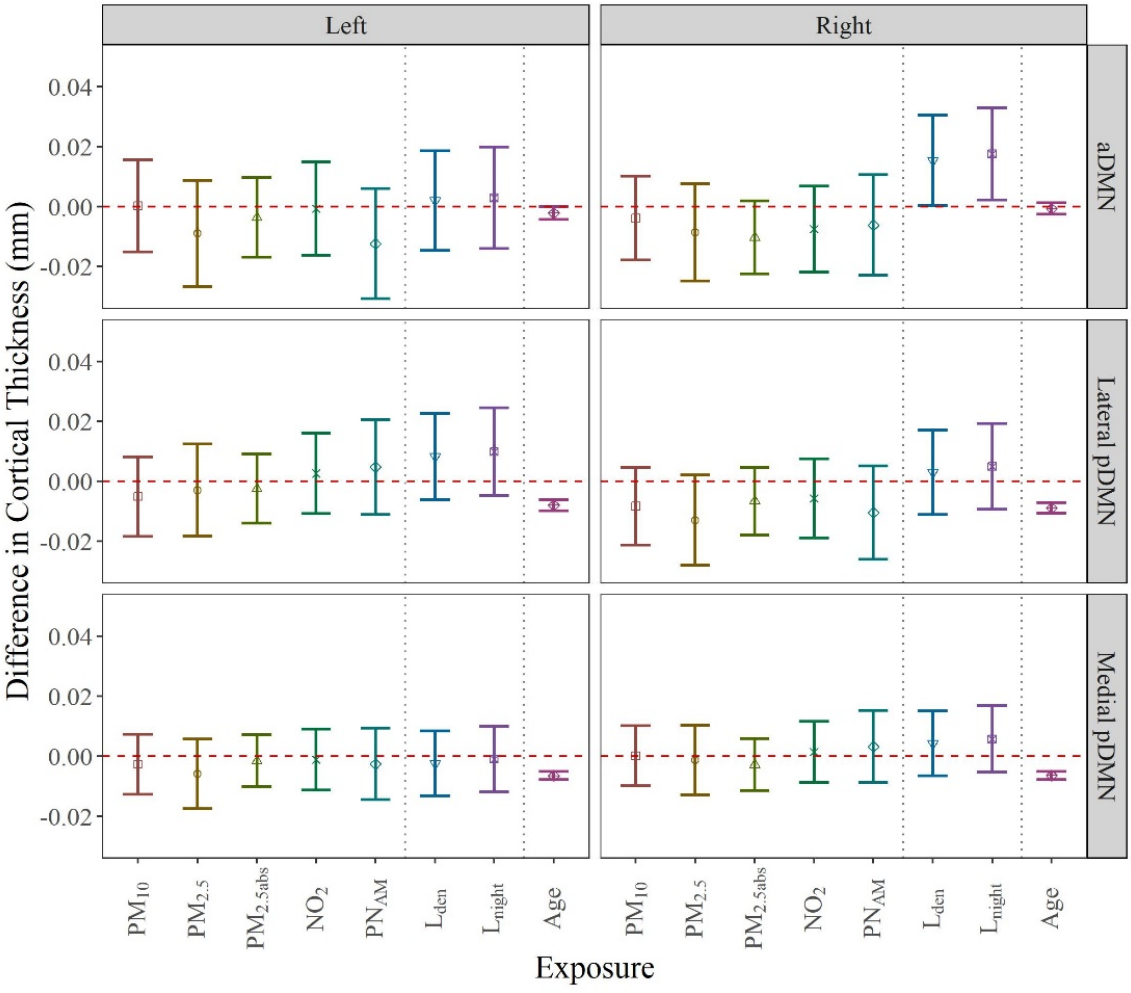

Figure 4. Associations between AP, noise, and change in cortical thickness (mm) within regions of the DMN in the right and left hemispheres of the brain. AP and noise estimates were calculated per IQR increase and per 10 dB(A), respectively, and are shown with 95% confidence intervals. Models were adjusted for age at MRI, sex, alcohol consumption, body mass index, diet, physical activity, smoking status, cumulative smoking, and environmental

tobacco smoke exposure. AP models were additionally adjusted for 24-hour outdoor noise and noise models were adjusted for $PM_{2.5abs}$. For reference, age at MRI and cortical thickness was also modeled, with associations estimated per 1-year increase and adjusted for sociodemographic variables included in the AP models as well as iSES and nSES.

Abbreviations: aDMN, anterior Default Mode Network; AP, air pollution; DMN, Default Mode Network; pDMN, posterior Default Mode Network; iSES, individual socioeconomic status; L_{den}, outdoor 24-hour weighted noise; L_{night}, outdoor nighttime noise; MRI, magnetic resonance imaging; NO_2, nitrogen dioxide; nSES, neighborhood socioeconomic status; PM_{10}, particulate matter with diameter ≤10 μm; $PM_{2.5}$, particulate matter with diameter ≤2.5 μm; $PM_{2.5abs}$, $PM_{2.5}$ absorbance; PN_{AM}, accumulation mode particle number concentration

In the multipollutant models, associations for lGI (Table S4) and cortical thickness (Table S5) were similar to those estimated in the single pollutant models, with the exception of lGI in the lateral pDMN. When restricting the analyses to the smaller group with complete indoor noise exposure data, we observed similar associations for both outdoor and indoor noise exposures (Fig. S4). Positive associations between outdoor noise and cortical thickness in the right aDMN were also reflected in the indoor estimates. For lGI in the aDMN as well as for cortical thickness in the left lateral pDMN, indoor noise associations were attenuated compared to the positive associations observed for outdoor exposures.

3.3 Effect Modification

For age, no consistent differences were apparent for lGI in the aDMN and medial pDMN (Fig. S5a). In the right lateral pDMN, most AP exposures were weakly positively associated with lGI among older participants but not younger participants. There were no clear variations in the association between AP and cortical thickness by age, though inverse associations with AP were observed only for younger participants in the left aDMN (Fig. S5b). For noise, we observed that increased outdoor noise was positively associated with cortical thickness in the lateral pDMN among younger participants whereas estimates were null or slightly negative for older participants.

3.4 Sensitivity Analyses

Addition of individual and neighborhood SES did not qualitatively alter the associations we estimated for lGI or cortical thickness (Fig. S3). Use of updated lifestyle variable data also did not affect the estimated associations (Table S6). When updating analyses to use exposures from participants' addresses at the 5-year HNR follow-up examination, we observed very similar estimates of association for lGI and cortical thickness as in the main analysis (Fig. S6). Similarly, restriction of the study population to those who did not move between baseline and 10-year HNR

follow-up (n=442) or to only those working less than 15 hours per week (n=429) did not result in large changes in the associations for lGI or cortical thickness (Fig. S6). Models using residential nearness to a major road (yes/no) broadly yielded weak negative associations with lGI and cortical thickness for those living close to major roads (Table S7).

4. Discussion

In a study of older adults within the 1000BRAINS study, we observed no strong associations between air pollution, noise, and brain structure measures of the DMN. Nevertheless, higher AP exposures were weakly associated with cortical thinning in the right aDMN and lateral pDMN with mixed results for noise. These results contribute to a small but growing literature investigating ambient environmental exposures and brain structure, while simultaneously confirming that connections between these exposures and the brain are complex and poorly understood at present.

4.1 Comparison to Prior Studies on AP and Brain Structure

Most studies connecting air pollution to brain health have focused primarily on measures of cognitive function. AP exposure has been linked to impaired cognitive development among children (D'Angiulli, 2018) as well as faster cognitive decline among adults (e.g., Kulick et al., 2020; Tzivian et al., 2015; Weuve et al., 2012). Additionally, epidemiologic studies have shown associations between AP and increased risk of neurodegenerative diseases such as Alzheimer's and dementia (Carey et al., 2018; Chen et al., 2017; Oudin et al., 2018). At present, studies on AP exposures and structural parameters of the brain are limited and have focused predominantly on volumetric measures (e.g., white matter volume [WMV], gray matter volume [GMV], total volume) or white matter hyperintensities. Most studies have observed decreases in one or more measures of brain volume with increased AP exposure (e.g., lower GMV and WMV in Casanova et al., 2016, lower WMV in Chen et al., 2015), with some variability by exposure and brain region. For example, in four studies within the UK Biobank, NO_2 exposure was associated with lower total GMV (Erickson et al., 2020) and prefrontal cortex volume (Gale et al., 2020), but not with GMV in the hippocampus (Hedges et al., 2019) or thalamus (Hedges et al., 2020). Windows of exposure also ranged from 2-year (Kulick et al., 2017) up to 17-year cumulative average exposure prior to MRI (Power et al., 2018).

To our knowledge, the only prior study to investigate AP and lGI was also conducted within the 1000BRAINS study and observed weak negative associations between AP exposures and lGI in the posterior regions of the fronto-parietal network (Nußbaum et al., 2020). AP and cortical thickness has been investigated in two recent studies on adults (Cho et al., 2020; Crous-Bou et al., 2020). In 957 adults, Cho et al. (2020) found that AP was associated with cortical thinning in frontal and temporal brain regions together with cortical thickening in occipital and cingulate brain regions. Within a cohort of healthy middle-aged adults with increased risk of Alzheimer's Disease (AD), Crous-Bou et al. (2020) observed associations between AP and cortical thinning in most AD-associated brain areas. Our results support these results that AP may be linked to cortical thinning in certain regions of the brain, but future studies investigating AP and brain structure using longitudinal data are needed to evaluate whether these associations represent true AP-induced changes in brain structures over time.

Unlike most prior studies, we focused on a specific functionally-defined network rather than using a whole-brain or anatomically-defined approach. The Default Mode Network is one of the most studied functional brain networks and plays an important role in memory recall as well as self-referential thought (Raichle, 2015). Within aging research, typical age-related changes in the deactivation of the DMN have been observed (Hafkemeijer et al., 2012). Additionally, the DMN is of particular interest in aging research because it is known to undergo atrophy, changes in functional connectivity (e.g., the PASA theory), and amyloid deposition with increasing age (Hafkemeijer et al., 2012).

When comparing our lGI results to patterns observed with aging, we observed no clear associations between AP, noise, and lGI as well as no evidence supporting a PASA pattern in the associations, which had been observed for AP and lGI levels in the fronto-parietal network (Nußbaum et al., 2020). This may be due to differences in the activation patterns of the two networks, as the DMN is most active during resting states whereas the fronto-parietal network is most active during externally-focused tasks. When considering our cortical thickness results and aging, the inverse associations between AP and cortical thickness in several regions of the right aDMN align with the right hemi-aging model (Brown and Jaffe, 1975; Dolcos et al., 2002). Nevertheless, like with lGI, we observed no pattern of association consistent with the PASA theory for cortical thickness.

While changes in cortical thickness and lGI can both be used to assess brain atrophy and both decrease with age (Hogstrom et al., 2013), it is not entirely surprising that we observed

different patterns of associations between the two, as prior studies have shown them to be uncorrelated or weakly negatively correlated (Gautam et al., 2015). This may be due to the fact that while cortical thickness reflects gray matter, lGI is a measure dependent on both gray and white matter. While it is not fully clear what AP-induced decreases in one measure but not in the other means for cognition or brain function, future studies should use several measures of brain structure in order to better understand how AP and noise may be influencing both white and gray matter in the brain (Hogstrom et al., 2013). Furthermore, few studies have analyzed how AP exposure may influence the patterns of functional communication in the brain (Pujol et al., 2016a; Pujol et al., 2016b). As brain signaling occurs both within networks as well as between networks, further studies are needed on how environmental exposures may affect both types of communication and whether AP-induced changes in brain structure are also reflected in changes in functional connectivity.

4.2 Noise

Chronic noise is an important environmental exposure that is known to cause adverse health effects, including increased risk of cardiovascular disease (Münzel et al., 2018), sleep disturbances (Basner et al., 2014), and depression (Hegewald et al., 2020; Orban et al., 2016). Nevertheless, very few epidemiologic studies have evaluated how long-term noise exposures may influence adult brain structure (Cheng et al., 2019; Crous-Bou et al., 2020; Nußbaum et al., 2020). In Cheng et al. (2019), fighter jet pilots had lower hippocampal GMV and worse working memory compared to matched controls. Using data from a healthy middle-aged cohort with increased AD risk, Crous-Bou et al. (2020) observed no statistically significant associations between noise and hippocampal volume, ventricle volume, or cortical thickness in brain regions vulnerable to AD. Contrary to expected, Nussbaum et al. (2020) observed positive associations between chronic outdoor noise and lGI in some regions of the fronto-parietal network. Nevertheless, indoor noise was not considered in the Nussbaum et al. (2020) study.

We observed positive associations between outdoor noise exposures and structural brain measures in several areas of the brain, with the strongest associations present for the aDMN. These results align with those seen by Nussbaum et al. (2020), where the positive associations were also observed primarily in the frontal regions of the brain. Nevertheless, in most cases, the positive associations we observed for outdoor noise exposures were attenuated for indoor exposures. Differences between outdoor and indoor noise estimates may also be due to

systematic differences in window type and use for persons with high noise exposure (e.g., more noise-proof windows and less time with windows open for highly exposed participants) that are only accounted for in the indoor noise estimates.

While little is known about noise and brain structure, some evidence exists showing that higher noise levels may be associated with decreased cognitive function, particularly among children (Clark and Paunovic, 2018). Studies on adults are more limited, particularly investigating long-term noise exposures, but the evidence seems to support that chronic noise exposure is associated with decreased cognitive function (Cheng et al., 2019; Fuks et al., 2019; Nußbaum et al., 2020; Tzivian et al., 2016b). While these studies do not provide evidence for direct comparison to our results on brain structure, they do support the hypothesis that environmental noise exposures may be important determinants of brain health and therefore influential in shaping morphological parameters.

4.3 Potential Mechanisms

Air pollution is hypothesized to influence health through several main pathways: first, by initiating local inflammatory processes in the lungs that can spawn systemic inflammation under chronic exposure; secondly, by direct translocation of small particles across the alveoli and into the blood stream, where they can travel and damage organs across the body; and thirdly, through activation and dysregulation of the autonomic nervous system (Block and Calderón-Garcidueñas, 2009). In recent years, evidence has emerged that small particles may also be able to enter into the brain directly via the olfactory bulb (Oberdörster et al., 2004). Systemic inflammation and circulating air pollutants are known to interact with the blood brain barrier, including the diffusion of cytokines across it and the initiation of neuroinflammatory cascades (Genc et al., 2012). Neuroinflammation is a hallmark of several neurologic diseases (e.g., Alzheimer's disease, Parkinson's Disease) as well as being associated with neuronal damage and decreases in white matter volume (Allen et al., 2017; Block and Calderón-Garcidueñas, 2009). Direct deposition of AP particles in the brain via the olfactory bulb may also result in the chronic activation of microglial cells and subsequently chronic production of pro-inflammatory species and oxidative stress (Block and Calderón-Garcidueñas, 2009; Block and Hong, 2005). With chronic AP exposure, these mechanisms may lead to structural changes in the brain. At present, it remains unclear as to why AP exposure may affect certain regions but not others in the brain.

One possible explanation for effects in frontal regions is through the direct deposition of particles via the olfactory bulb pathway.

Noise exposure is hypothesized to adversely influence human health through somewhat different pathways than AP. It is known that chronic noise exposure increases levels of annoyance and stress, which can activate the autonomic nervous system/hypothalamus-pituitary-adrenal axis (Jafari et al., 2019). Noise may also influence health by decreasing sleep quality and subsequently negatively affecting metabolism (Basner et al., 2014). At present, the ways by which noise exposure may influence brain structure remains unknown. Some possibilities include the induction of persistent tau pathology and altered auditory input that may cause changes in the hippocampus and cortex (Paul et al., 2019); increases in stress-induced free radicals, which may go on to affect cell morphology; increased glucocorticoids that can alter synaptic terminal structures and inhibit neuronal regeneration in some regions; and alterations in neurotransmitters that may affect synaptic plasticity (Arjunan and Rajan, 2020). Chronic noise has also been linked to increased risk of cardiovascular disease, which is associated with decreased cognitive function (Barnes, 2015). Lower cardiorespiratory fitness, which may result from disease, has also been associated with faster rates of brain atrophy (Barnes, 2015). As mentioned above, the mixed associations we observed for noise exposures, lGI, and cortical thickness may be due to error in exposure estimation, but it may also reflect compensatory mechanisms in certain areas of the brain. Should noise adversely affect other areas that have not been investigated up to this point, increased or non-changing lGI values in certain areas may reflect compensatory mechanisms on the part of the brain in order to offset the damage elsewhere. Further studies are needed looking at long-term effects of noise, particularly low-level chronic noise, on the brain in order to better understand the mix of positive and negative associations we observed in our study.

4.4 Study Strengths and Weaknesses

There are several limitations to our study. While the exposures were modeled for periods prior to the MRI examinations and ought to represent long-term exposures, we cannot draw longitudinal, causal conclusions as we do not have MRI data at baseline and therefore cannot identify exactly when any AP-associated structural changes may have occurred. Exposure misclassification in our exposures also exists, as they are modeled exposures and participants spent time other places than their home address. Nevertheless, sensitivity analyses restricted to those who did not move over the study period or were not working showed no qualitative change

in our results. Some of the AP exposures are highly correlated and, even after conducting multipollutant models, it is difficult to tease out which air pollutant may have be most strongly associated with brain structure. Future analyses including greenspace may also be of interest. Our indoor noise estimates were calculated based on behavior and window information collected via questionnaire and therefore have not been validated with on-site measurements. The study population in this study is also small and it is likely that we are somewhat underpowered to fully evaluate potential associations, particularly in the effect modification analyses. Nevertheless, efforts to obtain AP and noise exposure information for the HNR MultiGeneration Study participants in the 1000BRAINS Study are currently being planned and would result in an almost doubling of available participants for analysis. The results from this study should also be considered in the context participants' air pollution exposure levels, which while higher than recommended by the 2005 WHO guidelines (World Health Organization Occupational and Environmental Health Team, 2006), are lower than those observed in other regions of the world, including much of Asia and the Middle East. Establishment of cohorts with AP, noise, and MRI data in areas with higher exposure levels would provide insight whether and what kind of dose-response relationship may exist between AP and structural brain measures.

Our study also has several strengths. First, the 1000BRAINS study includes rich demographic and lifestyle data, which allowed us to adjust for many potential confounders. We were also able to leverage extensive exposure data to evaluate several novel exposures, including PN_{AM}. Few prior studies have investigated whether chronic noise exposures influence brain structure or whether quasi-ultrafine particles may be particularly influential due to their ability to pass through the olfactory bulb. This is also one of the first studies to adjust for chronic noise, a potentially important co-exposure from traffic, when estimating the association between AP and brain structure. Finally, we focused in this study on brain structural measures within an important functional network of the brain, a strategy which has not been employed in many prior studies and will hopefully inform future studies on environmental exposures and functional connectivity in the brain. As mentioned previously, future studies with long-term follow-up periods are needed to better understand how long-term AP may influence brain health over the lifespan and help elucidate potential causal pathways. There also remains a need for studies with information on several aspects of brain health, such that the interplay between air pollution, structural measures, functional connectivity, and neurological diseases (e.g., Alzheimer's disease) can be examined together within the same participants.

4.5 Conclusion

Overall, long-term air pollution and noise exposures were not consistently associated with the structural brain measures of lGI and cortical thickness within the DMN, with the exception of weak negative associations between AP and cortical thickness in the right hemisphere. As few prior studies exist on environmental exposures and brain structure within functional networks, further studies into how AP and noise may alter both brain structure as well as brain signaling are needed to better understand the role the environment plays in affecting human health across the whole body.

Acknowledgements: We thank the North Rhine-Westphalia State Agency for Nature, Environment and Consumer Protection (LANUV) for providing emission and land use data for North Rhine-Westphalia. We are indebted to the investigative group and the study personnel of the Heinz Nixdorf Recall (HNR) study and the 1000BRAINS study. We also thank the Heinz Nixdorf Foundation for the generous support of this study. The HNR study was supported by grants from the German Research Council (Deutsche Forschungsgemeinschaft; grants ER 155/6-1, ER 155/6-2, SI 236/8-1, and SI 236/9-1) and the Kulturstiftung Essen, Germany. The exposure assessment was funded through the European Community's Seventh Framework Program (FP7/ 2007–2011; grant 211250) and by the German Research Council (DFG; HO 3314/4-3). Further, this project was partially funded by the 1000BRAINS-Study of the Institute of Neuroscience and Medicine, Research Centre Jülich, Germany, and has received funding from the European Union's Horizon 2020 Research and Innovation Programme under grant agreement no. 945539 (HBP SGA3; S.C.) as well as from the Initiative and Networking Fund of the Helmholtz Association (S.C.).

5. References

Allen, J.L., Klocke, C., Morris-Schaffer, K., Conrad, K., Sobolewski, M., Cory-Slechta, D.A., 2017. Cognitive Effects of Air Pollution Exposures and Potential Mechanistic Underpinnings. Current environmental health reports 4, 180–191. https://doi.org/10.1007/s40572-017-0134-3.

Arjunan, A., Rajan, R., 2020. Noise and brain. Physiology & behavior 227, 113136. https://doi.org/10.1016/j.physbeh.2020.113136.

Barnes, J.N., 2015. Exercise, cognitive function, and aging. Advances in Physiology Education 39, 55–62. https://doi.org/10.1152/advan.00101.2014.

Basner, M., Babisch, W., Davis, A., Brink, M., Clark, C., Janssen, S., Stansfeld, S., 2014. Auditory and non-auditory effects of noise on health. The Lancet 383, 1325–1332. https://doi.org/10.1016/S0140-6736(13)61613-X.

Beckmann, C.F., DeLuca, M., Devlin, J.T., Smith, S.M., 2005. Investigations into resting-state connectivity using independent component analysis. Philosophical transactions of the Royal Society of London. Series B, Biological sciences 360, 1001–1013. https://doi.org/10.1098/rstb.2005.1634.

Beelen, R., Hoek, G., Vienneau, D., Eeftens, M., Dimakopoulou, K., Pedeli, X., Tsai, M.-Y., Künzli, N., Schikowski, T., Marcon, A., Eriksen, K.T., Raaschou-Nielsen, O., Stephanou, E., Patelarou, E., Lanki, T., Yli-Tuomi, T., Declercq, C., Falq, G., Stempfelet, M., Birk, M., Cyrys, J., Klot, S.v., Nádor, G., Varró, M.J., Dėdelė, A., Gražulevičienė, R., Mölter, A., Lindley, S., Madsen, C., Cesaroni, G., Ranzi, A., Badaloni, C., Hoffmann, B., Nonnemacher, M., Krämer, U., Kuhlbusch, T., Cirach, M., Nazelle, A. de, Nieuwenhuijsen, M., Bellander, T., Korek, M., Olsson, D., Strömgren, M., Dons, E., Jerrett, M., Fischer, P., Wang, M., Brunekreef, B., Hoogh, K. de, 2013. Development of NO2 and NOx land use regression models for estimating air pollution exposure in 36 study areas in Europe – The ESCAPE project. Atmospheric Environment 72, 10–23. https://doi.org/10.1016/j.atmosenv.2013.02.037.

Birmili, W., Weinhold, K., Rasch, F., Sonntag, A., Sun, J., Merkel, M., Wiedensohler, A., Bastian, S., Schladitz, A., Löschau, G., Cyrys, J., Pitz, M., Gu, J., Kusch, T., Flentje, H., Quass, U., Kaminski, H., Kuhlbusch, T.A.J., Meinhardt, F., Schwerin, A., Bath, O., Ries, L., Gerwig, H., Wirtz, K., Fiebig, M., 2016. Long-term observations of tropospheric particle number size distributions and equivalent black carbon mass concentrations in the German

727 Ultrafine Aerosol Network (GUAN). Earth Syst. Sci. Data 8, 355–382.
728 https://doi.org/10.5194/essd-8-355-2016.
729 Block, M.L., Calderón-Garcidueñas, L., 2009. Air pollution: mechanisms of neuroinflammation
730 and CNS disease. Trends in neurosciences 32, 506–516.
731 https://doi.org/10.1016/j.tins.2009.05.009.
732 Block, M.L., Hong, J.-S., 2005. Microglia and inflammation-mediated neurodegeneration:
733 multiple triggers with a common mechanism. Progress in neurobiology 76, 77–98.
734 https://doi.org/10.1016/j.pneurobio.2005.06.004.
735 Brown, J.W., Jaffe, J., 1975. Hypothesis on cerebral dominance. Neuropsychologia 13, 107–110.
736 https://doi.org/10.1016/0028-3932(75)90054-8.
737 Bundesministerium der Justiz, 2006. Vorläufige Berechnungsmethode Für Den Umgebungslärm
738 an StraBen (VBUS)., in: Bundesanzeiger, 154a, pp. 30–49.
739 Carey, I.M., Anderson, H.R., Atkinson, R.W., Beevers, S.D., Cook, D.G., Strachan, D.P.,
740 Dajnak, D., Gulliver, J., Kelly, F.J., 2018. Are noise and air pollution related to the incidence
741 of dementia? A cohort study in London, England. BMJ open 8, e022404.
742 https://doi.org/10.1136/bmjopen-2018-022404.
743 Casanova, R., Wang, X., Reyes, J., Akita, Y., Serre, M.L., Vizuete, W., Chui, H.C., Driscoll, I.,
744 Resnick, S.M., Espeland, M.A., Chen, J.-C., 2016. A Voxel-Based Morphometry Study
745 Reveals Local Brain Structural Alterations Associated with Ambient Fine Particles in Older
746 Women. Frontiers in human neuroscience 10, 495.
747 https://doi.org/10.3389/fnhum.2016.00495.
748 Caspers, S., Moebus, S., Lux, S., Pundt, N., Schütz, H., Mühleisen, T.W., Gras, V., Eickhoff,
749 S.B., Romanzetti, S., Stöcker, T., Stirnberg, R., Kirlangic, M.E., Minnerop, M., Pieperhoff,
750 P., Mödder, U., Das, S., Evans, A.C., Jöckel, K.-H., Erbel, R., Cichon, S., Nöthen, M.M.,
751 Sturma, D., Bauer, A., Jon Shah, N., Zilles, K., Amunts, K., 2014. Studying variability in
752 human brain aging in a population-based German cohort-rationale and design of
753 1000BRAINS. Frontiers in aging neuroscience 6, 149.
754 https://doi.org/10.3389/fnagi.2014.00149.
755 Chen, H., Kwong, J.C., Copes, R., Hystad, P., van Donkelaar, A., Tu, K., Brook, J.R., Goldberg,
756 M.S., Martin, R.V., Murray, B.J., Wilton, A.S., Kopp, A., Burnett, R.T., 2017. Exposure to
757 ambient air pollution and the incidence of dementia: A population-based cohort study.
758 Environment international 108, 271–277. https://doi.org/10.1016/j.envint.2017.08.020.

759 Chen, J.-C., Wang, X., Wellenius, G.A., Serre, M.L., Driscoll, I., Casanova, R., McArdle, J.J.,
760 Manson, J.E., Chui, H.C., Espeland, M.A., 2015. Ambient air pollution and neurotoxicity on
761 brain structure: Evidence from women's health initiative memory study. Annals of neurology
762 78, 466–476. https://doi.org/10.1002/ana.24460.
763 Cheng, H., Sun, G., Li, M., Yin, M., Chen, H., 2019. Neuron loss and dysfunctionality in
764 hippocampus explain aircraft noise induced working memory impairment: a resting-state
765 fMRI study on military pilots. Bioscience trends 13, 430–440.
766 https://doi.org/10.5582/bst.2019.01190.
767 Cho, J., Noh, Y., Kim, S.Y., Sohn, J., Noh, J., Kim, W., Cho, S.-K., Seo, H., Seo, G., Lee, S.-K.,
768 Seo, S., Koh, S.-B., Oh, S.S., Kim, H.J., Seo, S.W., Shin, D.-S., Kim, N., Kim, H.H., Lee, J.I.,
769 Kim, C., 2020. Long-Term Ambient Air Pollution Exposures and Brain Imaging Markers in
770 Korean Adults: The Environmental Pollution-Induced Neurological EFfects (EPINEF) Study.
771 Environ Health Perspect 128, 117006. https://doi.org/10.1289/EHP7133.
772 Clark, C., Paunovic, K., 2018. WHO Environmental Noise Guidelines for the European Region:
773 A Systematic Review on Environmental Noise and Cognition. International journal of
774 environmental research and public health 15. https://doi.org/10.3390/ijerph15020285.
775 Crous-Bou, M., Gascon, M., Gispert, J.D., Cirach, M., Sánchez-Benavides, G., Falcon, C.,
776 Arenaza-Urquijo, E.M., Gotsens, X., Fauria, K., Sunyer, J., Nieuwenhuijsen, M.J., Luis
777 Molinuevo, J., 2020. Impact of urban environmental exposures on cognitive performance and
778 brain structure of healthy individuals at risk for Alzheimer's dementia. Environment
779 international 138, 105546. https://doi.org/10.1016/j.envint.2020.105546.
780 Cyrys, J., Eeftens, M., Heinrich, J., Ampe, C., Armengaud, A., Beelen, R., Bellander, T.,
781 Beregszaszi, T., Birk, M., Cesaroni, G., Cirach, M., Hoogh, K. de, Nazelle, A. de, Vocht, F.
782 de, Declercq, C., Dėdelė, A., Dimakopoulou, K., Eriksen, K., Galassi, C., Grąulevičienė, R.,
783 Grivas, G., Gruzieva, O., Gustafsson, A.H., Hoffmann, B., Iakovides, M., Ineichen, A.,
784 Krämer, U., Lanki, T., Lozano, P., Madsen, C., Meliefste, K., Modig, L., Mölter, A., Mosler,
785 G., Nieuwenhuijsen, M., Nonnemacher, M., Oldenwening, M., Peters, A., Pontet, S., Probst-
786 Hensch, N., Quass, U., Raaschou-Nielsen, O., Ranzi, A., Sugiri, D., Stephanou, E.G.,
787 Taimisto, P., Tsai, M.-Y., Vaskövi, É., Villani, S., Wang, M., Brunekreef, B., Hoek, G., 2012.
788 Variation of NO2 and NOx concentrations between and within 36 European study areas:
789 Results from the ESCAPE study. Atmospheric Environment 62, 374–390.
790 https://doi.org/10.1016/j.atmosenv.2012.07.080.

Dale, A.M., Fischl, B., Sereno, M.I., 1999. Cortical surface-based analysis: I. Segmentation and surface reconstruction. NeuroImage 9, 179–194. https://doi.org/10.1006/nimg.1998.0395.

D'Angiulli, A., 2018. Severe Urban Outdoor Air Pollution and Children's Structural and Functional Brain Development, From Evidence to Precautionary Strategic Action. Frontiers in public health 6, 95. https://doi.org/10.3389/fpubh.2018.00095.

DataKustik GmbH. CadnaA.

Davis, S.W., Dennis, N.A., Daselaar, S.M., Fleck, M.S., Cabeza, R., 2008. Que PASA? The posterior-anterior shift in aging. Cerebral cortex (New York, N.Y. : 1991) 18, 1201–1209. https://doi.org/10.1093/cercor/bhm155.

Dolcos, F., Rice, H.J., Cabeza, R., 2002. Hemispheric asymmetry and aging: right hemisphere decline or asymmetry reduction. Neuroscience & Biobehavioral Reviews 26, 819–825. https://doi.org/10.1016/S0149-7634(02)00068-4.

Dragano, N., Hoffmann, B., Stang, A., Moebus, S., Verde, P.E., Weyers, S., Möhlenkamp, S., Schmermund, A., Mann, K., Jöckel, K.-H., Erbel, R., Siegrist, J., 2009. Subclinical coronary atherosclerosis and neighbourhood deprivation in an urban region. Eur J Epidemiol 24, 25–35. https://doi.org/10.1007/s10654-008-9292-9.

Eeftens, M., Beelen, R., Hoogh, K. de, Bellander, T., Cesaroni, G., Cirach, M., Declercq, C., Dėdelė, A., Dons, E., Nazelle, A. de, Dimakopoulou, K., Eriksen, K., Falq, G., Fischer, P., Galassi, C., Gražulevičienė, R., Heinrich, J., Hoffmann, B., Jerrett, M., Keidel, D., Korek, M., Lanki, T., Lindley, S., Madsen, C., Mölter, A., Nádor, G., Nieuwenhuijsen, M., Nonnemacher, M., Pedeli, X., Raaschou-Nielsen, O., Patelarou, E., Quass, U., Ranzi, A., Schindler, C., Stempfelet, M., Stephanou, E., Sugiri, D., Tsai, M.-Y., Yli-Tuomi, T., Varró, M.J., Vienneau, D., Klot, S.v., Wolf, K., Brunekreef, B., Hoek, G., 2012. Development of Land Use Regression models for PM(2.5), PM(2.5) absorbance, PM(10) and PM(coarse) in 20 European study areas; results of the ESCAPE project. Environmental science & technology 46, 11195–11205. https://doi.org/10.1021/es301948k.

Erickson, L.D., Gale, S.D., Anderson, J.E., Brown, B.L., Hedges, D.W., 2020. Association between Exposure to Air Pollution and Total Gray Matter and Total White Matter Volumes in Adults: A Cross-Sectional Study. Brain sciences 10. https://doi.org/10.3390/brainsci10030164.

European Environment Agency, 2002. Directive 2002/49/EC of the European Parliament and of the Council of 25 June 2002 relating to the assessment and management of environmental noise. Official Journal European Communities, 12–25.

European Parliament, Council of the European Union, 2008. Directive 2008/50/EC of the European Parliament and of the Council of 21 May 2008 on ambient air quality and cleaner air for Europe. Official Journal of the European Union L152, 1–44.

Fischl, B., Dale, A.M., 2000. Measuring the thickness of the human cerebral cortex from magnetic resonance images. Proceedings of the National Academy of Sciences of the United States of America 97, 11050–11055. https://doi.org/10.1073/pnas.200033797.

Fischl, B., Sereno, M.I., Dale, A.M., 1999. Cortical surface-based analysis. II: Inflation, flattening, and a surface-based coordinate system. NeuroImage 9, 195–207. https://doi.org/10.1006/nimg.1998.0396.

Foraster, M., Künzli, N., Aguilera, I., Rivera, M., Agis, D., Vila, J., Bouso, L., Deltell, A., Marrugat, J., Ramos, R., Sunyer, J., Elosua, R., Basagaña, X., 2014. High blood pressure and long-term exposure to indoor noise and air pollution from road traffic. Environ Health Perspect 122, 1193–1200. https://doi.org/10.1289/ehp.1307156.

Fuks, K.B., Wigmann, C., Altug, H., Schikowski, T., 2019. Road Traffic Noise at the Residence, Annoyance, and Cognitive Function in Elderly Women. International journal of environmental research and public health 16. https://doi.org/10.3390/ijerph16101790.

Gale, S.D., Erickson, L.D., Anderson, J.E., Brown, B.L., Hedges, D.W., 2020. Association between exposure to air pollution and prefrontal cortical volume in adults: A cross-sectional study from the UK biobank. Environmental research 185, 109365. https://doi.org/10.1016/j.envres.2020.109365.

Gautam, P., Anstey, K.J., Wen, W., Sachdev, P.S., Cherbuin, N., 2015. Cortical gyrification and its relationships with cortical volume, cortical thickness, and cognitive performance in healthy mid-life adults. Behavioural brain research 287, 331–339. https://doi.org/10.1016/j.bbr.2015.03.018.

Genc, S., Zadeoglulari, Z., Fuss, S.H., Genc, K., 2012. The adverse effects of air pollution on the nervous system. Journal of toxicology 2012, 782462. https://doi.org/10.1155/2012/782462.

Hafkemeijer, A., van der Grond, J., Rombouts, S.A.R.B., 2012. Imaging the default mode network in aging and dementia. Biochimica et biophysica acta 1822, 431–441. https://doi.org/10.1016/j.bbadis.2011.07.008.

853 Hedges, D.W., Erickson, L.D., Gale, S.D., Anderson, J.E., Brown, B.L., 2020. Association
854 between exposure to air pollution and thalamus volume in adults: A cross-sectional study.
855 PloS one 15, e0230829. https://doi.org/10.1371/journal.pone.0230829.
856 Hedges, D.W., Erickson, L.D., Kunzelman, J., Brown, B.L., Gale, S.D., 2019. Association
857 between exposure to air pollution and hippocampal volume in adults in the UK Biobank.
858 Neurotoxicology 74, 108–120. https://doi.org/10.1016/j.neuro.2019.06.005.
859 Hegewald, J., Schubert, M., Freiberg, A., Romero Starke, K., Augustin, F., Riedel-Heller, S.G.,
860 Zeeb, H., Seidler, A., 2020. Traffic Noise and Mental Health: A Systematic Review and
861 Meta-Analysis. International journal of environmental research and public health 17.
862 https://doi.org/10.3390/ijerph17176175.
863 Hennig, F., Sugiri, D., Tzivian, L., Fuks, K., Moebus, S., Jöckel, K.-H., Vienneau, D.,
864 Kuhlbusch, T., Hoogh, K. de, Memmesheimer, M., Jakobs, H., Quass, U., Hoffmann, B.,
865 2016. Comparison of Land-Use Regression Modeling with Dispersion and Chemistry
866 Transport Modeling to Assign Air Pollution Concentrations within the Ruhr Area.
867 Atmosphere 7, 48. https://doi.org/10.3390/atmos7030048.
868 Hogstrom, L.J., Westlye, L.T., Walhovd, K.B., Fjell, A.M., 2013. The structure of the cerebral
869 cortex across adult life: age-related patterns of surface area, thickness, and gyrification.
870 Cerebral cortex (New York, N.Y. : 1991) 23, 2521–2530.
871 https://doi.org/10.1093/cercor/bhs231.
872 Jafari, Z., Kolb, B.E., Mohajerani, M.H., 2019. Noise exposure accelerates the risk of cognitive
873 impairment and Alzheimer's disease: Adulthood, gestational, and prenatal mechanistic
874 evidence from animal studies. Neuroscience and biobehavioral reviews.
875 https://doi.org/10.1016/j.neubiorev.2019.04.001.
876 Jenkinson, M., Beckmann, C.F., Behrens, T.E.J., Woolrich, M.W., Smith, S.M., 2012. FSL.
877 NeuroImage 62, 782–790. https://doi.org/10.1016/j.neuroimage.2011.09.015.
878 Jockwitz, C., Caspers, S., Lux, S., Jütten, K., Schleicher, A., Eickhoff, S.B., Amunts, K., Zilles,
879 K., 2017. Age- and function-related regional changes in cortical folding of the default mode
880 network in older adults. Brain structure & function 222, 83–99.
881 https://doi.org/10.1007/s00429-016-1202-4.
882 Jockwitz, C., Mérillat, S., Liem, F., Oschwald, J., Amunts, K., Caspers, S., Jäncke, L., 2019.
883 Generalizing age effects on brain structure and cognition: A two-study comparison approach.
884 Human brain mapping. https://doi.org/10.1002/hbm.24524.

Kulick, E.R., Elkind, M.S., Boehme, A.K., Joyce, N.R., Schupf, N., Kaufman, J.D., Mayeux, R., Manly, J.J., Wellenius, G.A., 2020. Long-term exposure to ambient air pollution, APOE-ε4 status, and cognitive decline in a cohort of older adults in northern Manhattan. Environment international 136, 105440. https://doi.org/10.1016/j.envint.2019.105440.

Kulick, E.R., Wellenius, G.A., Kaufman, J.D., DeRosa, J.T., Kinney, P.L., Cheung, Y.K., Wright, C.B., Sacco, R.L., Elkind, M.S., 2017. Long-Term Exposure to Ambient Air Pollution and Subclinical Cerebrovascular Disease in NOMAS (the Northern Manhattan Study). Stroke 48, 1966–1968. https://doi.org/10.1161/STROKEAHA.117.016672.

Lucht, S., Hennig, F., Moebus, S., Führer-Sakel, D., Herder, C., Jöckel, K.-H., Hoffmann, B., 2019. Air pollution and diabetes-related biomarkers in non-diabetic adults: A pathway to impaired glucose metabolism? Environment international 124, 370–392. https://doi.org/10.1016/j.envint.2019.01.005.

Memmesheimer, M., Friese, E., Ebel, A., Jakobs, H.J., Feldmann, H., Kessler, C., Piekorz, G., 2004. Long-term simulations of particulate matter in Europe on different scales using sequential nesting of a regional model. IJEP 22, 5530, 108. https://doi.org/10.1504/IJEP.2004.005530.

Münzel, T., Schmidt, F.P., Steven, S., Herzog, J., Daiber, A., Sørensen, M., 2018. Environmental Noise and the Cardiovascular System. Journal of the American College of Cardiology 71, 688–697. https://doi.org/10.1016/j.jacc.2017.12.015.

Nonnemacher, M., Jakobs, H., Viehmann, A., Vanberg, I., Kessler, C., Moebus, S., Möhlenkamp, S., Erbel, R., Hoffmann, B., Memmesheimer, M., 2014. Spatio-temporal modelling of residential exposure to particulate matter and gaseous pollutants for the Heinz Nixdorf Recall Cohort. Atmospheric Environment 91, 15–23. https://doi.org/10.1016/j.atmosenv.2014.03.052.

Nußbaum, R., Lucht, S., Jockwitz, C., Moebus, S., Engel, M., Jöckel, K.-H., Caspers, S., Hoffmann, B., 2020. Associations of Air Pollution and Noise with Local Brain Structure in a Cohort of Older Adults. Environmental health perspectives 128, 67012. https://doi.org/10.1289/EHP5859.

Oberdörster, G., Sharp, Z., Atudorei, V., Elder, A., Gelein, R., Kreyling, W., Cox, C., 2004. Translocation of inhaled ultrafine particles to the brain. Inhalation toxicology 16, 437–445. https://doi.org/10.1080/08958370490439597.

Ohlwein, S., Hennig, F., Lucht, S., Matthiessen, C., Pundt, N., Moebus, S., Jöckel, K.-H., Hoffmann, B., 2019. Indoor and outdoor road traffic noise and incident diabetes mellitus. Environmental Epidemiology 3, e037. https://doi.org/10.1097/EE9.0000000000000037.

Orban, E., McDonald, K., Sutcliffe, R., Hoffmann, B., Fuks, K.B., Dragano, N., Viehmann, A., Erbel, R., Jöckel, K.-H., Pundt, N., Moebus, S., 2016. Residential Road Traffic Noise and High Depressive Symptoms after Five Years of Follow-up: Results from the Heinz Nixdorf Recall Study. Environmental health perspectives 124, 578–585. https://doi.org/10.1289/ehp.1409400.

Oudin, A., Segersson, D., Adolfsson, R., Forsberg, B., 2018. Association between air pollution from residential wood burning and dementia incidence in a longitudinal study in Northern Sweden. PloS one 13, e0198283. https://doi.org/10.1371/journal.pone.0198283.

Paul, K.C., Haan, M., Mayeda, E.R., Ritz, B.R., 2019. Ambient Air Pollution, Noise, and Late-Life Cognitive Decline and Dementia Risk. Annual review of public health 40, 203–220. https://doi.org/10.1146/annurev-publhealth-040218-044058.

Power, M.C., Lamichhane, A.P., Liao, D., Xu, X., Jack, C.R., Gottesman, R.F., Mosley, T., Stewart, J.D., Yanosky, J.D., Whitsel, E.A., 2018. The Association of Long-Term Exposure to Particulate Matter Air Pollution with Brain MRI Findings: The ARIC Study. Environmental health perspectives 126, 27009. https://doi.org/10.1289/EHP2152.

Pujol, J., Fenoll, R., Macià, D., Martínez-Vilavella, G., Alvarez-Pedrerol, M., Rivas, I., Forns, J., Deus, J., Blanco-Hinojo, L., Querol, X., Sunyer, J., 2016a. Airborne copper exposure in school environments associated with poorer motor performance and altered basal ganglia. Brain and behavior 6, e00467. https://doi.org/10.1002/brb3.467.

Pujol, J., Martínez-Vilavella, G., Macià, D., Fenoll, R., Alvarez-Pedrerol, M., Rivas, I., Forns, J., Blanco-Hinojo, L., Capellades, J., Querol, X., Deus, J., Sunyer, J., 2016b. Traffic pollution exposure is associated with altered brain connectivity in school children. NeuroImage 129, 175–184. https://doi.org/10.1016/j.neuroimage.2016.01.036.

Raichle, M.E., 2015. The brain's default mode network. Annual review of neuroscience 38, 433–447. https://doi.org/10.1146/annurev-neuro-071013-014030.

Schaer, M., Cuadra, M.B., Schmansky, N., Fischl, B., Thiran, J.-P., Eliez, S., 2012. How to measure cortical folding from MR images: a step-by-step tutorial to compute local gyrification index. Journal of visualized experiments : JoVE, e3417. https://doi.org/10.3791/3417.

948 Schmermund, A., Möhlenkamp, S., Stang, A., Grönemeyer, D., Seibel, R., Hirche, H., Mann, K.,
949 Siffert, W., Lauterbach, K., Siegrist, J., Jöckel, K.-H., Erbel, R., 2002. Assessment of
950 clinically silent atherosclerotic disease and established and novel risk factors for predicting
951 myocardial infarction and cardiac death in healthy middle-aged subjects: Rationale and design
952 of the Heinz Nixdorf RECALL Study. American Heart Journal 144, 212–218.
953 https://doi.org/10.1067/mhj.2002.123579.
954 Schraufnagel, D.E., Balmes, J.R., Cowl, C.T., Matteis, S. de, Jung, S.-H., Mortimer, K., Perez-
955 Padilla, R., Rice, M.B., Riojas-Rodriguez, H., Sood, A., Thurston, G.D., To, T., Vanker, A.,
956 Wuebbles, D.J., 2019. Air Pollution and Noncommunicable Diseases: A Review by the
957 Forum of International Respiratory Societies' Environmental Committee, Part 2: Air Pollution
958 and Organ Systems. Chest 155, 417–426. https://doi.org/10.1016/j.chest.2018.10.041.
959 Stang, A., Moebus, S., Dragano, N., Beck, E.M., Möhlenkamp, S., Schmermund, A., Siegrist, J.,
960 Erbel, R., Jöckel, K.H., 2005. Baseline recruitment and analyses of nonresponse of the Heinz
961 Nixdorf recall study: Identifiability of phone numbers as the major determinant of response.
962 Eur J Epidemiol 20, 489–496. https://doi.org/10.1007/s10654-005-5529-z.
963 Textor, J., Hardt, J., Knüppel, S., 2011. DAGitty: a graphical tool for analyzing causal diagrams.
964 Epidemiology (Cambridge, Mass.) 22, 745. https://doi.org/10.1097/EDE.0b013e318225c2be.
965 Thurston, G.D., Kipen, H., Annesi-Maesano, I., Balmes, J., Brook, R.D., Cromar, K., Matteis, S.
966 de, Forastiere, F., Forsberg, B., Frampton, M.W., Grigg, J., Heederik, D., Kelly, F.J., Kuenzli,
967 N., Laumbach, R., Peters, A., Rajagopalan, S.T., Rich, D., Ritz, B., Samet, J.M., Sandstrom,
968 T., Sigsgaard, T., Sunyer, J., Brunekreef, B., 2017. A joint ERS/ATS policy statement: what
969 constitutes an adverse health effect of air pollution? An analytical framework. The European
970 respiratory journal 49. https://doi.org/10.1183/13993003.00419-2016.
971 Tonne, C., Elbaz, A., Beevers, S., Singh-Manoux, A., 2014. Traffic-related air pollution in
972 relation to cognitive function in older adults. Epidemiology (Cambridge, Mass.) 25, 674–681.
973 https://doi.org/10.1097/EDE.0000000000000144.
974 Tsapanou, A., Habeck, C., Gazes, Y., Razlighi, Q., Sakhardande, J., Stern, Y., Salthouse, T.A.,
975 2019. Brain biomarkers and cognition across adulthood. Human brain mapping 40, 3832–
976 3842. https://doi.org/10.1002/hbm.24634.
977 Tzivian, L., Dlugaj, M., Winkler, A., Hennig, F., Fuks, K., Sugiri, D., Schikowski, T., Jakobs, H.,
978 Erbel, R., Jöckel, K.-H., Moebus, S., Hoffmann, B., Weimar, C., 2016a. Long-term air
979 pollution and traffic noise exposures and cognitive function:A cross-sectional analysis of the

Heinz Nixdorf Recall study. Journal of toxicology and environmental health. Part A 79, 1057–1069. https://doi.org/10.1080/15287394.2016.1219570.

Tzivian, L., Dlugaj, M., Winkler, A., Weinmayr, G., Hennig, F., Fuks, K.B., Vossoughi, M., Schikowski, T., Weimar, C., Erbel, R., Jöckel, K.-H., Moebus, S., Hoffmann, B., 2016b. Long-Term Air Pollution and Traffic Noise Exposures and Mild Cognitive Impairment in Older Adults: A Cross-Sectional Analysis of the Heinz Nixdorf Recall Study. Environmental health perspectives 124, 1361–1368. https://doi.org/10.1289/ehp.1509824.

Tzivian, L., Winkler, A., Dlugaj, M., Schikowski, T., Vossoughi, M., Fuks, K., Weinmayr, G., Hoffmann, B., 2015. Effect of long-term outdoor air pollution and noise on cognitive and psychological functions in adults. International journal of hygiene and environmental health 218, 1–11. https://doi.org/10.1016/j.ijheh.2014.08.002.

UNESCO, 1997. International Standard Classification of Education ISCED 1997. UNITED NATIONS EDUCATIONAL, SCIENTIFIC AND CULTURAL ORGANIZATION, 49 pp.

Weuve, J., Puett, R.C., Schwartz, J., Yanosky, J.D., Laden, F., Grodstein, F., 2012. Exposure to particulate air pollution and cognitive decline in older women. Archives of internal medicine 172, 219–227. https://doi.org/10.1001/archinternmed.2011.683.

WHO Regional Office for Europe, 2009. Night noise guidelines for Europe. World Health Organization, Copenhagen, 162 pp. https://www.euro.who.int/en/health-topics/environment-and-health/noise/publications/2009/night-noise-guidelines-for-europe.

Wilker, E.H., Martinez-Ramirez, S., Kloog, I., Schwartz, J., Mostofsky, E., Koutrakis, P., Mittleman, M.A., Viswanathan, A., 2016. Fine Particulate Matter, Residential Proximity to Major Roads, and Markers of Small Vessel Disease in a Memory Study Population. Journal of Alzheimer's disease : JAD 53, 1315–1323. https://doi.org/10.3233/JAD-151143.

Wilker, E.H., Preis, S.R., Beiser, A.S., Wolf, P.A., Au, R., Kloog, I., Li, W., Schwartz, J., Koutrakis, P., DeCarli, C., Seshadri, S., Mittleman, M.A., 2015. Long-term exposure to fine particulate matter, residential proximity to major roads and measures of brain structure. Stroke 46, 1161–1166. https://doi.org/10.1161/STROKEAHA.114.008348.

Winkler, G., Döring, A., 1995. Kurzmethoden zur Charakterisierung des Ernährungsmusters: Einsatz und Auswertung eines Food-Frequency-Fragebogens. Ernährungs-Umschau 42, 289–291.

Winkler, G., Döring, A., 1998. Validation of a short qualitative food frequency list used in several German large scale surveys. Zeitschrift fur Ernahrungswissenschaft 37, 234–241.

World Health Organization, 2018. Environmental Noise Guidelines for the European Region. World Health Organization, Copenhagen, 181 pp. https://www.euro.who.int/__data/assets/pdf_file/0008/383921/noise-guidelines-eng.pdf (accessed 2 August 2021).

World Health Organization Occupational and Environmental Health Team, 2006. WHO Air quality guidelines for particulate matter, ozone, nitrogen dioxide and sulfur dioxide: Global update 2005. World Health Organization, Geneva, Switzerland, 22 pp. https://apps.who.int/iris/handle/10665/69477 (accessed 7 March 2019).

Wright, B., Peters, E., Ettinger, U., Kuipers, E., Kumari, V., 2014. Understanding noise stress-induced cognitive impairment in healthy adults and its implications for schizophrenia. Noise & health 16, 166–176. https://doi.org/10.4103/1463-1741.134917.

Supplemental Material

Title: Long-term Air Pollution, Noise, and Structural Measures of the Default Mode Network in the Brain: Results from the 1000BRAINS Cohort

Authors: Sarah Lucht, Lina Glaubitz, Susanne Moebus, Sara Schramm, Christiane Jockwitz, Svenja Caspers, and Barbara Hoffmann.

Table of Contents

Table S1. Comparison of baseline sociodemographic, exposure, and outcome characteristics for all participants at the 10-year HNR follow-up examination (n=3,087), the 1000BRAINS participants included (n=579) in the analyses, and the 1000BRAINS participants excluded from current analyses (n=109). All variables were collected for the HNR baseline examination (2000-2003), except for age at MRI, lGI, and cortical thickness.

Variable	Attendees of 10-year HNR Examination (n=3,087) Mean ± SD or Median [IQR] or n (%)	Included (n=579) Mean ± SD or Median [IQR] or n (%)	Excluded (n=109)	
			Mean ± SD or Median [IQR] or n (%)	Missing (n)
Age at HNR Baseline (years)	58.4 ± 7.3	56.2 ± 6.7	57.2 ± 7.2	0
Age at MRI (years)		66.5 ± 6.7	67.6 ± 7.1	0
BMI (kg/m^2)	27.5 ± 4.4	27.3 ± 4.1	27.1 ± 3.8	1
Neighborhood Unemployment (%)	12.3 ± 3.4	12.1 ± 3.3	12.6 ± 3.3	0
Cumulative Smoking (pack-years)	19.3 [28.0]	18.8 [25.0]	16.1 [25.9]	9
Sex, Female	1,580 (51.2)	265 (45.8)	40 (36.7)	0
Formal Education				0
≤10 years	266 (8.6)	32 (5.5)	5 (4.6)	-
11-13 years	1,698 (55.0)	302 (52.2)	54 (49.5)	-
14-17 years	725 (23.5)	143 (24.7)	34 (31.2)	-
≥18 years	394 (12.8)	102 (17.6)	16 (14.7)	-
Physical Activity, Yes	1,833 (59.4)	362 (62.5)	71 (65.1)	0
Smoking Status				0
Never Smoker	1,348 (43.7)	250 (43.2)	44 (40.4)	-
Former Smoker	1,127 (36.5)	214 (37.0)	45 (41.3)	-
Current Smoker	612 (19.8)	115 (19.9)	20 (18.3)	-
Environmental Tobacco Smoke Exposure, Yes	1,085 (35.1)	225 (38.9)	32 (29.0)	0
Alcohol Consumption (Drinks/Week)				7
Never	1,418 (45.9)	226 (39.0)	29 (28.4)	-
1 to 3	486 (15.7)	96 (16.6)	12 (11.8)	-
>3 to 6	345 (11.1)	80 (13.8)	16 (15.7)	-
>6 to 14	396 (12.8)	87 (15.0)	23 (22.5)	-
>14	388 (12.6)	90 (15.5)	22 (21.6)	-
Diet				4
Unfavorable Diet	1,132 (36.7)	235 (40.6)	52 (49.5)	-
Normal Diet	1,067 (34.6)	209 (36.1)	28 (26.7)	-
Favorable Diet	846 (27.4)	135 (23.3)	25 (23.8)	-
Environmental Exposures				
PM_{10} ($\mu g/m^3$)	27.7 ± 1.9	27.5 ± 1.8	27.7 ± 1.7	0
$PM_{2.5}$ ($\mu g/m^3$)	18.4 ± 1.1	18.2 ± 1.0	18.4 ± 1.0	0
$PM_{2.5abs}$ (0.0001/m)	1.6 ± 0.4	1.5 ± 0.4	1.6 ± 0.3	0
NO_2 ($\mu g/m^3$)	30.1 ± 4.9	29.5 ± 4.6	30.1 ± 4.9	0
PN_{AM} (n/mL)	3,756.5 ± 444.6	3,725 ± 435	3777.4 ± 461.7	0
O-L_{den} (dB[A])	54.0 ± 8.7	53.4 ± 8.4	54.3 ± 8.2	2
O-L_{night} (db[A])	45.0 ± 8.6	44.4 ± 8.3	45.3 ± 8.1	2
I- L_{den} (dB[A])	34.7 ± 14.2	35.1 ± 12.5	33.4 ± 12.7	13
I-L_{night} (dB[A])	28.0 ± 14.0	27.3 ± 13.8	27.3 ± 14.8	13
lGI				
Left aDMN		2.0 ± 0.1	2.0 ± 0.1	76
Left Medial pDMN		2.8 ± 0.2	2.8 ± 0.1	76
Left Lateral pDMN		3.0 ± 0.1	3.0 ± 0.1	76
Right aDMN		2.1 ± 0.1	2.1 ± 0.1	85

Right Medial pDMN		2.9 ± 0.2	2.8 ± 0.2	85
Right Lateral pDMN		3.0 ± 0.1	3.0 ± 0.1	85
Cortical Thickness (mm)				
Left aDMN		2.4 ± 0.2	2.5 ± 0.1	72
Left Medial pDMN		2.2± 0.1	2.2 ± 0.1	72
Left Lateral pDMN		2.4 ± 0.1	2.4 ± 0.2	72
Right aDMN		2.4 ± 0.1	2.5 ± 0.1	72
Right Medial pDMN		2.2 ± 0.1	2.2 ± 0.1	72
Right Lateral pDMN		2.5 ± 0.2	2.5 ± 0.2	72

Abbreviations: aDMN, anterior Default Mode Network; BMI, body mass index; HNR, Heinz Nixdorf Recall; I-L_{den}, indoor 24-hour weighted noise; I-L_{night}, indoor nighttime noise; IQR, interquartile range; lGI, local gyrification index; MRI, magnetic resonance imaging; NO_2, nitrogen dioxide; O-L_{den}, outdoor 24-hour weighted noise; O-L_{night}, outdoor nighttime noise; pDMN, posterior Default Mode Network; PM_{10}, particulate matter with diameter ≤10 µm; $PM_{2.5}$, particulate matter with diameter ≤2.5 µm; $PM_{2.5abs}$, $PM_{2.5}$ absorbance; PN_{AM}, accumulation mode particle number concentration; SD, standard deviation

Table S2. Spearman correlations between long-term air pollution and chronic traffic noise exposures.

	PM_{10}	$PM_{2.5}$	$PM_{2.5abs}$	NO_2	PN_{AM}	L_{den}	L_{night}	$I\text{-}L_{den}$	$I\text{-}L_{night}$
PM_{10}	1	0.91	0.91	0.54	0.49	0.23	0.24	0.12	0.15
$PM_{2.5}$		1	0.89	0.64	0.72	0.24	0.24	0.11	0.14
$PM_{2.5abs}$			1	0.61	0.52	0.40	0.41	0.22	0.25
NO_2				1	0.57	0.30	0.30	0.14	0.19
PN_{AM}					1	0.20	0.22	0.08	0.11
L_{den}						1	0.99	0.50	0.40
L_{night}							1	0.50	0.40
$I\text{-}L_{den}$								1	0.40
$I\text{-}L_{night}$									1

Abbreviations: $I\text{-}L_{den}$, indoor 24-hour weighted noise; $I\text{-}L_{night}$, indoor nighttime noise; NO_2, nitrogen dioxide; L_{den}, outdoor 24-hour weighted noise; L_{night}, outdoor nighttime noise; PM_{10}, particulate matter with diameter ≤10 μm; $PM_{2.5}$, particulate matter with diameter ≤2.5 μm; $PM_{2.5abs}$, $PM_{2.5}$ absorbance; PN_{AM}, accumulation mode particle number concentration

Table S3. Description of brain structure measures (lGI, cortical thickness) in the three regions of the DMN across both hemispheres.

	Left Mean ± SD	**Right** Mean ± SD
lGI		
aDMN	2.0 ± 0.1	2.1 ± 0.1
Medial pDMN	2.8 ± 0.2	2.9 ± 0.2
Lateral pDMN	3.0 ± 0.1	3.0 ± 0.1
Cortical Thickness (mm)		
aDMN	2.4 ± 0.2	2.4 ± 0.1
Medial pDMN	2.2 ± 0.1	2.2 ± 0.1
Lateral pDMN	2.4 ± 0.1	2.5 ± 0.1

Abbreviations: aDMN, anterior Default Mode Network; lGI, local gyrification index; pDMN, posterior Default Mode Network; SD, standard deviation

Table S4. Associations between an IQR increase in air pollution and lGI, adjusted for Main Model covariates, in the Main Model as well as in multipollutant models adjusting separately for NO_2, PN_{AM}, and $PM_{2.5}$.

Air Pollutant	Main Model	Adj. for NO_2	Adj. for PN_{AM}	Adj. for $PM_{2.5}$
Left aDMN				
PM_{10} (μg/m^3)	-0.006 (-0.014, 0.002)	-0.004 (-0.013, 0.006)	-0.006(-0.015, 0.003)	-
$PM_{2.5}$ (μg/m^3)	-0.006 (-0.016, 0.004)	-0.002 (-0.014, 0.010)	-0.006 (-0.019, 0.007)	-
$PM_{2.5abs}$ (0.0001/m)	-0.003 (-0.010, 0.004)	0.002 (-0.008, 0.011)	-0.002 (-0.010, 0.006)	-
NO_2 (μg/m^3)	-0.007 (-0.015, 0.002)	-	-0.007 (-0.016, 0.003)	-0.006 (-0.016, 0.005)
PN_{AM} (n/mL)	-0.004 (-0.014, 0.006)	-0.001 (-0.012, 0.011)	-	0.000 (-0.013, 0.014)
Left Lateral pDMN				
PM_{10} (μg/m^3)	0.001 (-0.012, 0.013)	0.004 (-0.011, 0.018)	0.000 (-0.014, 0.014)	-
$PM_{2.5}$ (μg/m^3)	0.002 (-0.012, 0.017)	0.008 (-0.010, 0.027)	0.002 (-0.018, 0.022)	-
$PM_{2.5abs}$ (0.0001/m)	0.010 (-0.001, 0.021)	0.023 (0.008, 0.038)	0.011 (-0.001, 0.023)	-
NO_2 (μg/m^3)	-0.004 (-0.017, 0.009)	-	-0.007 (-0.021, 0.008)	-0.009 (-0.025, 0.007)
PN_{AM} (n/mL)	0.002 (-0.013, 0.017)	0.005 (-0.012, 0.023)	-	0.000 (-0.020, 0.021)
Left Medial pDMN				
PM_{10} (μg/m^3)	-0.001 (-0.016, 0.015)	0.002 (-0.016, 0.020)	-0.002 (-0.019, 0.014)	-
$PM_{2.5}$ (μg/m^3)	0.003 (-0.015, 0.021)	0.009 (-0.013, 0.031)	0.001 (-0.024, 0.025)	-
$PM_{2.5abs}$ (0.0001/m)	-0.002 (-0.015, 0.012)	0.001 (-0.018, 0.019)	-0.003 (-0.018, 0.011)	-
NO_2 (μg/m^3)	-0.004 (-0.020, 0.012)	-	-0.007 (-0.025, 0.011)	-0.008 (-0.028, 0.011)
PN_{AM} (n/mL)	0.004 (-0.014, 0.023)	0.008 (-0.013, 0.029)	-	0.004 (-0.021, 0.029)
Right aDMN				
PM_{10} (μg/m^3)	-0.005 (-0.013, 0.003)	-0.005 (-0.015, 0.005)	-0.005 (-0.014, 0.004)	-
$PM_{2.5}$ (μg/m^3)	-0.003 (-0.013, 0.006)	-0.003 (-0.015, 0.009)	-0.003 (-0.016, 0.010)	-
$PM_{2.5abs}$ (0.0001/m)	0.001 (-0.006, 0.008)	0.004 (-0.006, 0.014)	0.002 (-0.006, 0.009)	-
NO_2 (μg/m^3)	-0.002 (-0.011, 0.006)	-	-0.002 (-0.011, 0.008)	-0.001 (-0.011, 0.010)
PN_{AM} (n/mL)	-0.003 (-0.013, 0.008)	-0.002 (-0.013, 0.010)	-	0.000 (-0.014, 0.013)
Right Lateral pDMN				
PM_{10} (μg/m^3)	-0.001 (-0.015, 0.013)	0.003 (-0.013, 0.019)	-0.005 (-0.019, 0.010)	-
$PM_{2.5}$ (μg/m^3)	0.004 (-0.012, 0.020)	0.013 (-0.007, 0.032)	-0.004 (-0.025, 0.017)	-
$PM_{2.5abs}$ (0.0001/m)	0.007 (-0.005, 0.019)	0.019 (0.003, 0.035)	0.005 (-0.008, 0.018)	-
NO_2 (μg/m^3)	-0.007 (-0.021, 0.007)	-	-0.013 (-0.029, 0.002)	-0.014 (-0.031, 0.004)
PN_{AM} (n/mL)	0.009 (-0.007, 0.026)	0.016 (-0.002, 0.035)	-	0.012 (-0.010, 0.034)
Right Medial pDMN				
PM_{10} (μg/m^3)	0.003 (-0.014, 0.020)	0.004 (-0.015, 0.023)	0.003 (-0.015, 0.021)	-
$PM_{2.5}$ (μg/m^3)	0.006 (-0.013, 0.026)	0.009 (-0.014, 0.033)	0.011 (-0.015, 0.037)	-
$PM_{2.5abs}$ (0.0001/m)	0.000 (-0.015, 0.014)	-0.007 (-0.020, 0.019)	-0.000 (-0.016, 0.015)	-
NO_2 (μg/m^3)	0.000 (-0.017, 0.017)	-	0.000 (-0.019, 0.019)	-0.005 (-0.025, 0.016)
PN_{AM} (n/mL)	0.000 (-0.019, 0.020)	0.000 (-0.022, 0.023)	-	-0.007 (-0.034, 0.020)

Abbreviations: aDMN, anterior Default Mode Network; lGI, local gyrification index; NO_2, nitrogen dioxide; pDMN, posterior Default Mode Network; PM_{10}, particulate matter with diameter ≤10 μm; $PM_{2.5}$, particulate matter with diameter ≤2.5 μm; $PM_{2.5abs}$, $PM_{2.5}$ absorbance; PN_{AM}, accumulation mode particle number concentration.

Table S5. Associations between an IQR increase in air pollution and cortical thickness (mm) in the Main Model as well as in multipollutant models additionally adjusting for NO_2, PN_{AM}, and $PM_{2.5}$ (individually).

Air Pollutant	Main Model	Adj. for NO_2	Adj. for PN_{AM}	Adj. for $PM_{2.5}$
Left aDMN				
PM_{10} ($\mu g/m^3$)	0.000 (-0.015, 0.016)	0.001 (-0.017, 0.018)	0.005 (-0.012, 0.022)	-
$PM_{2.5}$ ($\mu g/m^3$)	-0.009 (-0.027, 0.009)	-0.013 (-0.035, 0.009)	-0.002 (-0.026, 0.022)	-
$PM_{2.5abs}$ (0.0001/m)	-0.004 (-0.017, 0.010)	-0.006 (-0.024, 0.012)	-0.001 (-0.015, 0.014)	-
NO_2 ($\mu g/m^3$)	-0.001(-0.016, 0.015)	-	0.005 (-0.012, 0.023)	0.006 (-0.013, 0.025)
PN_{AM} (n/mL)	-0.012 (-0.031, 0.006)	-0.015 (-0.036, 0.005)	-	-0.011 (-0.036, 0.014)
Left Lateral pDMN				
PM_{10} ($\mu g/m^3$)	-0.005 (-0.018, 0.008)	-0.008 (-0.024, 0.007)	-0.008 (-0.022, 0.007)	-
$PM_{2.5}$ ($\mu g/m^3$)	-0.003 (-0.018, 0.013)	-0.007 (-0.026, 0.012)	-0.011 (-0.032, 0.010)	-
$PM_{2.5abs}$ (0.0001/m)	-0.002 (-0.014, 0.009)	-0.007 (-0.022, 0.008)	-0.004 (-0.016, 0.008)	-
NO_2 ($\mu g/m^3$)	0.003 (-0.011, 0.016)	-	0.001 (-0.014, 0.016)	0.006 (-0.010, 0.023)
PN_{AM} (n/mL)	0.005 (-0.011, 0.021)	0.004 (-0.014, 0.022)	-	0.012 (-0.009, 0.034)
Left Medial pDMN				
PM_{10} ($\mu g/m^3$)	-0.003 (-0.013, 0.007)	-0.003 (-0.014, 0.009)	-0.002 (-0.013, 0.009)	-
$PM_{2.5}$ ($\mu g/m^3$)	-0.006 (-0.017, 0.006)	-0.008 (-0.022, 0.007)	-0.008 (-0.023, 0.008)	-
$PM_{2.5abs}$ (0.0001/m)	-0.002 (-0.010, 0.007)	-0.002 (-0.013, 0.010)	-0.001 (-0.010, 0.008)	-
NO_2 ($\mu g/m^3$)	-0.001 (-0.011, 0.009)	-	0.000 (-0.012, 0.011)	0.003 (-0.010, 0.015)
PN_{AM} (n/mL)	-0.003 (-0.015, 0.009)	-0.002 (-0.016, 0.011)	-	0.003 (-0.014, 0.019)
Right aDMN				
PM_{10} ($\mu g/m^3$)	-0.004 (-0.018, 0.010)	0.000 (-0.016, 0.016)	-0.002 (-0.017, 0.013)	-
$PM_{2.5}$ ($\mu g/m^3$)	-0.009 (-0.025, 0.008)	-0.006 (-0.026, 0.015)	-0.008 (-0.030, 0.014)	-
$PM_{2.5abs}$ (0.0001/m)	-0.010 (-0.022, 0.002)	-0.011 (-0.027, 0.006)	-0.010 (-0.023, 0.003)	-
NO_2 ($\mu g/m^3$)	-0.008 (-0.022, 0.007)	-	-0.006 (-0.022, 0.010)	-0.005 (-0.022, 0.013)
PN_{AM} (n/mL)	-0.006 (-0.023, 0.011)	-0.003 (-0.022, 0.016)	-	0.000 (-0.023, 0.022)
Right Lateral pDMN				
PM_{10} ($\mu g/m^3$)	-0.008 (-0.021, 0.005)	-0.007 (-0.022, 0.008)	-0.006 (-0.020, 0.008)	-
$PM_{2.5}$ ($\mu g/m^3$)	-0.013 (-0.028, 0.002)	-0.014 (-0.032, 0.005)	-0.011 (-0.032, 0.009)	-
$PM_{2.5abs}$ (0.0001/m)	-0.007 (-0.018, 0.005)	-0.006 (-0.021, 0.009)	-0.004 (-0.017, 0.008)	-
NO_2 ($\mu g/m^3$)	-0.006 (-0.019, 0.008)	-	-0.002 (-0.017, 0.013)	0.001 (-0.015, 0.018)
PN_{AM} (n/mL)	-0.010 (-0.026, 0.005)	-0.009 (-0.027, 0.008)	-	-0.003 (-0.024, 0.018)
Right Medial pDMN				
PM_{10} ($\mu g/m^3$)	0.000 (-0.010, 0.010)	-0.001 (-0.012, 0.011)	-0.001 (-0.012, 0.010)	-
$PM_{2.5}$ ($\mu g/m^3$)	-0.001 (-0.013, 0.010)	-0.003 (-0.018, 0.011)	-0.006 (-0.022, 0.010)	-
$PM_{2.5abs}$ (0.0001/m)	-0.003 (-0.012, 0.006)	-0.006 (-0.018, 0.005)	-0.004 (-0.013, 0.005)	-
NO_2 ($\mu g/m^3$)	0.001 (-0.009, 0.012)	-	0.000 (-0.011, 0.012)	0.003 (-0.010, 0.016)
PN_{AM} (n/mL)	0.003 (-0.009, 0.015)	0.003 (-0.010, 0.017)	-	0.007 (-0.009, 0.024)

Abbreviations: aDMN, anterior Default Mode Network; lGI, local gyrification index; NO_2, nitrogen dioxide; pDMN, posterior Default Mode Network; PM_{10}, particulate matter with diameter ≤10 μm; $PM_{2.5}$, particulate matter with diameter ≤2.5 μm; $PM_{2.5abs}$, $PM_{2.5}$ absorbance; PN_{AM}, accumulation mode particle number concentration.

Table S6. Associations between environmental exposures, lGI, and cortical thickness (mm) in the Main Model as and the Main Model using updated sociodemographic variables from the 10-year HNR follow-up were used. Associations are given per IQR increase for air pollutants and per 10 dB(A) increase in noise.

	lGI		Cortical Thickness	
Exposure	Main Model	Updated Variables Model	Main Model	Updated Variables Model
Left aDMN				
PM_{10} (μg/m^3)	-0.006 (-0.014, 0.002)	-0.005 (-0.014, 0.003)	0.000 (-0.015, 0.016)	0.000 (-0.015, 0.016)
$PM_{2.5}$ (μg/m^3)	-0.006 (-0.016, 0.004)	-0.004 (-0.014, 0.005)	-0.009 (-0.027, 0.009)	-0.011 (-0.029, 0.007)
$PM_{2.5abs}$ (0.0001/m)	-0.003 (-0.010, 0.004)	-0.002 (-0.009, 0.005)	-0.004 (-0.017, 0.010)	-0.004 (-0.018, 0.009)
NO_2 (μg/m^3)	-0.007 (-0.015, 0.002)	-0.005 (-0.014, 0.003)	-0.001 (-0.016, 0.015)	-0.001 (-0.017, 0.014)
PN_{AM} (n/mL)	-0.004 (-0.014, 0.006)	-0.002 (-0.012, 0.008)	-0.012 (-0.031, 0.006)	-0.015 (-0.033, 0.003)
L_{den} (dB[A])	0.005 (-0.004, 0.014)	0.005 (-0.004, 0.014)	0.002 (-0.015, 0.019)	0.002 (-0.015, 0.018)
L_{night} (dB[A])	0.005 (-0.004, 0.014)	0.005 (-0.004, 0.014)	0.003 (-0.014, 0.020)	0.002 (-0.015, 0.020)
Left Lateral pDMN				
PM_{10} (μg/m^3)	0.001 (-0.012, 0.013)	-0.001 (-0.014, 0.012)	-0.005 (-0.018, 0.008)	-0.005 (-0.018, 0.008)
$PM_{2.5}$ (μg/m^3)	0.002 (-0.012, 0.017)	-0.000 (-0.015, 0.015)	-0.003 (-0.018, 0.013)	-0.004 (-0.019, 0.011)
$PM_{2.5abs}$ (0.0001/m)	0.010 (-0.001, 0.021)	0.009 (-0.002, 0.020)	-0.002 (-0.014, 0.009)	-0.004 (-0.016, 0.007)
NO_2 (μg/m^3)	-0.004 (-0.017, 0.009)	-0.004 (-0.017, 0.009)	0.003 (-0.011, 0.016)	0.001 (-0.013, 0.014)
PN_{AM} (n/mL)	0.002 (-0.013, 0.017)	0.001 (-0.014, 0.017)	0.005 (-0.011, 0.021)	0.003 (-0.013, 0.018)
L_{den} (dB[A])	-0.003 (-0.017, 0.011)	-0.005 (-0.019, 0.009)	0.008 (-0.006, 0.023)	0.007 (-0.007, 0.021)
L_{night} (dB[A])	-0.004 (-0.018, 0.010)	-0.005 (-0.019, 0.009)	0.010 (-0.005, 0.025)	0.009 (-0.006, 0.023)
Left Medial pDMN				
PM_{10} (μg/m^3)	-0.001 (-0.016, 0.015)	-0.002 (-0.017, 0.014)	-0.003 (-0.013, 0.007)	-0.004 (-0.014, 0.006)
$PM_{2.5}$ (μg/m^3)	0.003 (-0.015, 0.021)	0.002 (-0.016, 0.020)	-0.006 (-0.017, 0.006)	-0.008 (-0.019, 0.004)
$PM_{2.5abs}$ (0.0001/m)	-0.002 (-0.015, 0.012)	-0.002 (-0.016, 0.011)	-0.002 (-0.010, 0.007)	-0.003 (-0.012, 0.006)
NO_2 (μg/m^3)	-0.004 (-0.020, 0.012)	-0.004 (-0.020, 0.011)	-0.001 (-0.011, 0.009)	-0.002 (-0.012, 0.008)
PN_{AM} (n/mL)	0.004 (-0.014, 0.023)	0.004 (-0.014, 0.023)	-0.003 (-0.015, 0.009)	-0.003 (-0.015, 0.008)
L_{den} (dB[A])	0.005 (-0.012, 0.022)	0.005 (-0.012, 0.022)	-0.002 (-0.013, 0.008)	-0.003 (-0.014, 0.008)
L_{night} (dB[A])	0.005 (-0.012, 0.022)	0.005 (-0.012, 0.023)	-0.001 (-0.023, 0.010)	-0.001 (-0.012, 0.010)
Right aDMN				
PM_{10} (μg/m^3)	-0.005 (-0.013, 0.003)	-0.005 (-0.014, 0.003)	-0.004 (-0.018, 0.010)	-0.003 (-0.018, 0.011)
$PM_{2.5}$ (μg/m^3)	-0.003 (-0.013, 0.006)	-0.004 (-0.014, 0.006)	-0.009 (-0.025, 0.008)	-0.009 (-0.25, 0.007)
$PM_{2.5abs}$ (0.0001/m)	0.001 (-0.006, 0.008)	0.001 (-0.007, 0.008)	-0.010 (-0.022, 0.002)	-0.010 (-0.023, 0.002)
NO_2 (μg/m^3)	-0.002 (-0.011, 0.006)	-0.002 (-0.011, 0.006)	-0.008 (-0.022, 0.007)	-0.006 (-0.020, 0.008)
PN_{AM} (n/mL)	-0.003 (-0.013, 0.008)	-0.003 (-0.013, 0.007)	-0.006 (-0.023, 0.011)	-0.007 (-0.024, 0.009)
L_{den} (dB[A])	0.004 (-0.005, 0.013)	0.003 (-0.006, 0.012)	0.015 (0.000, 0.030)	0.015 (-0.000, 0.030)
L_{night} (dB[A])	0.003 (-0.006, 0.012)	0.003 (-0.007, 0.012)	0.018 (0.002, 0.033)	0.017 (0.002, 0.033)
Right Lateral pDMN				
PM_{10} (μg/m^3)	-0.001 (-0.015, 0.013)	-0.001 (-0.014, 0.013)	-0.008 (-0.021, 0.005)	-0.001 (-0.011, 0.009)
$PM_{2.5}$ (μg/m^3)	0.004 (-0.012, 0.020)	0.003 (-0.012, 0.019)	-0.013 (-0.028, 0.002)	-0.003 (-0.014, 0.009)
$PM_{2.5abs}$ (0.0001/m)	0.007 (-0.005, 0.019)	0.007 (-0.005, 0.018)	-0.007 (-0.018, 0.005)	-0.004 (-0.013, 0.005)
NO_2 (μg/m^3)	-0.007 (-0.021, 0.007)	-0.006 (-0.020, 0.008)	-0.006 (-0.019, 0.008)	0.001 (-0.009, 0.012)
PN_{AM} (n/mL)	0.009 (-0.007, 0.026)	0.009 (-0.007, 0.025)	-0.010 (-0.026, 0.005)	0.003 (-0.009, 0.015)
L_{den} (dB[A])	-0.005 (-0.020, 0.010)	-0.005 (-0.020, 0.009)	0.003 (-0.011, 0.017)	0.004 (-0.007, 0.015)
L_{night} (dB[A])	-0.005 (-0.020, 0.010)	-0.005 (-0.020, 0.010)	0.005 (-0.009, 0.019)	0.006 (-0.005, 0.017)
Right Medial pDMN				
PM_{10} (μg/m^3)	0.003 (-0.014, 0.020)	0.002 (-0.015, 0.019)	0.000 (-0.010, 0.010)	-0.009 (-0.022, 0.004)
$PM_{2.5}$ (μg/m^3)	0.006 (-0.013, 0.026)	0.005 (-0.014, 0.024)	-0.001 (-0.013, 0.010)	-0.014 (-0.029, 0.001)
$PM_{2.5abs}$ (0.0001/m)	0.000 (-0.015, 0.014)	-0.002 (-0.016, 0.013)	-0.003 (-0.012, 0.006)	-0.008 (-0.020, 0.003)
NO_2 (μg/m^3)	0.000 (-0.017, 0.017)	-0.001 (-0.018, 0.016)	0.001 (-0.009, 0.012)	-0.007 (-0.020, 0.006)
PN_{AM} (n/mL)	0.000 (-0.019, 0.020)	0.000 (-0.019, 0.020)	0.003 (-0.009, 0.015)	-0.011 (-0.026, 0.005)
L_{den} (dB[A])	-0.006 (-0.024, 0.012)	-0.007 (-0.025, 0.011)	0.004 (-0.007, 0.015)	0.002 (-0.012, 0.016)
L_{night} (dB[A])	-0.007 (-0.025, 0.011)	-0.008 (-0.026, 0.011)	0.006 (-0.005, 0.017)	0.005 (-0.009, 0.019)

Abbreviations: aDMN, anterior Default Mode Network; L_{den}, weighted 24-hour noise; lGI, local gyrification index; L_{night}, nighttime noise; NO_2, nitrogen dioxide; pDMN, posterior Default Mode Network; PM_{10}, particulate matter with diameter ≤10 μm; $PM_{2.5}$, particulate matter with diameter ≤2.5 μm; $PM_{2.5abs}$, $PM_{2.5}$ absorbance; PN_{AM}, accumulation mode particle number concentration.

Table S7. Associations between residential nearness to a major road (n_{yes}=109; n_{no}=470) and brain structure measures (lGI and cortical thickness) in various regions of the Default Mode Network. Models were adjusted for age at MRI, sex, alcohol consumption, body mass index, diet, physical activity, smoking status, cumulative smoking, environmental tobacco smoke exposure, and 24-hour outdoor noise.

Region of the DMN	**Left** Estimate (95% CI)	**Right** Estimate (95% CI)
lGI		
aDMN	-0.005 (-0.028, 0.018)	0.015 (-0.008, 0.039)
Lateral pDMN	-0.006 (-0.042, 0.030)	-0.021 (-0.059, 0.017)
Medial pDMN	-0.016 (-0.060, 0.027)	0.008 (-0.039, 0.054)
Cortical Thickness (mm)		
aDMN	-0.004 (-0.047, 0.039)	-0.012 (-0.051, 0.027)
Lateral pDMN	-0.019 (-0.056, 0.018)	-0.014 (-0.050, 0.022)
Medial pDMN	-0.006 (-0.034, 0.022)	-0.008 (-0.036, 0.020)

Abbreviations: aDMN, anterior Default Mode Network; CI, confidence interval; DMN, Default Mode Network; lGI, local gyrification index; MRI, magnetic resonance imaging; pDMN, posterior Default Mode Network.

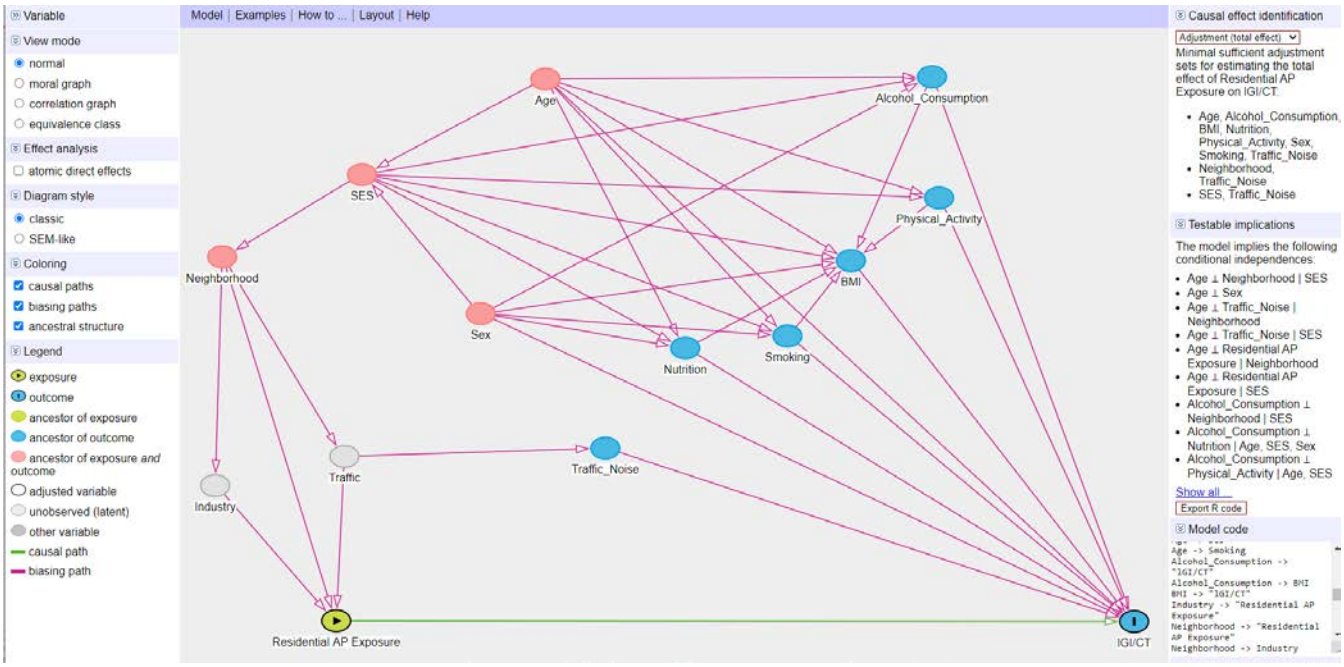

Fig. S1. Directed acyclic graph constructed using DAGitty depicting the causal assumptions made when evaluating the associations between AP and structural measures of the Default Mode Network of the brain (lGI, CT). Minimum adjustment sets for addressing potential confounding on AP and DMN measures were: 1) Age, Alcohol Consumption, BMI, Nutrition, Physical Activity, Sex, Smoking, Traffic Noise; 2) Neighborhood, Traffic Noise; 3) individual SES, Traffic Noise.

Abbreviations: AP, air pollution; BMI, body mass index; CT, cortical thickness; DMN, Default Mode Network; lGI, local gyrification index; SES, socioeconomic status

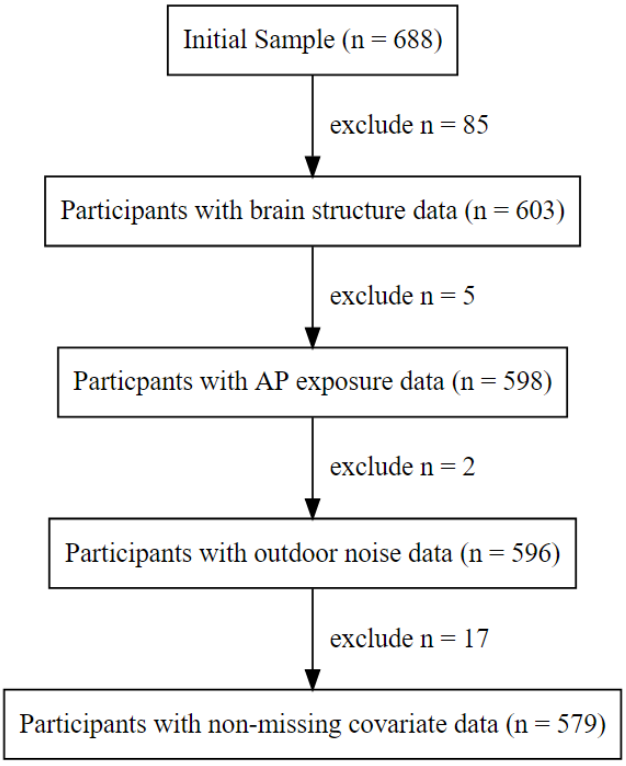

Fig. S2. Derivation of the study population.

Abbreviations: AP, air pollution

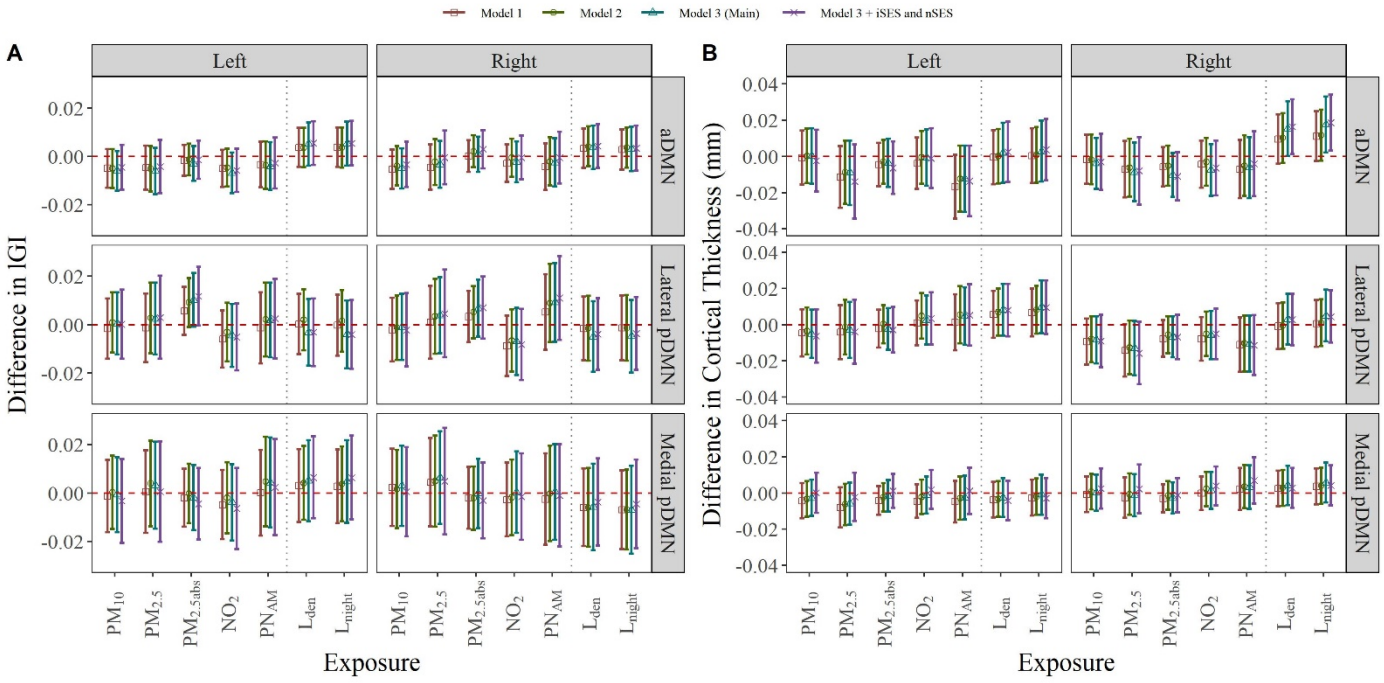

Fig. S3. Associations between air pollution, noise, and A) lGI and B) cortical thickness in the DMN of the brain, upon adjustment for various different variables. Estimates and their 95% confidence intervals were calculated per interquartile range increase for AP and per 10 dB(A) for noise exposures. Model 1 included the AP or noise exposure, age and sex. Model 2 included age, sex, body mass index, alcohol consumption, smoking status, cumulative smoking, environmental tobacco smoke exposure, diet, and physical activity. In Model 3 (Main Model), AP models were additionally adjusted for outdoor L_{den} whereas noise models were additionally adjusted for $PM_{2.5abs}$. A further model adjusting for Model 3 variables as well as individual and neighborhood socioeconomic status was also conducted.

Abbreviations: aDMN, anterior Default Mode Network; AP, air pollution; dB(A), A-weighted decibels; DMN, Default Mode Network; L_{den}, outdoor 24-hour weighted noise; lGI, local gyrification index; L_{night}, outdoor nighttime noise; NO_2, nitrogen dioxide; pDMN, posterior Default Mode Network; PM_{10}, particulate matter with diameter ≤10 µm; $PM_{2.5}$, particulate matter with diameter ≤2.5 µm; $PM_{2.5abs}$, $PM_{2.5}$ absorbance; PN_{AM}, accumulation mode particle number concentration

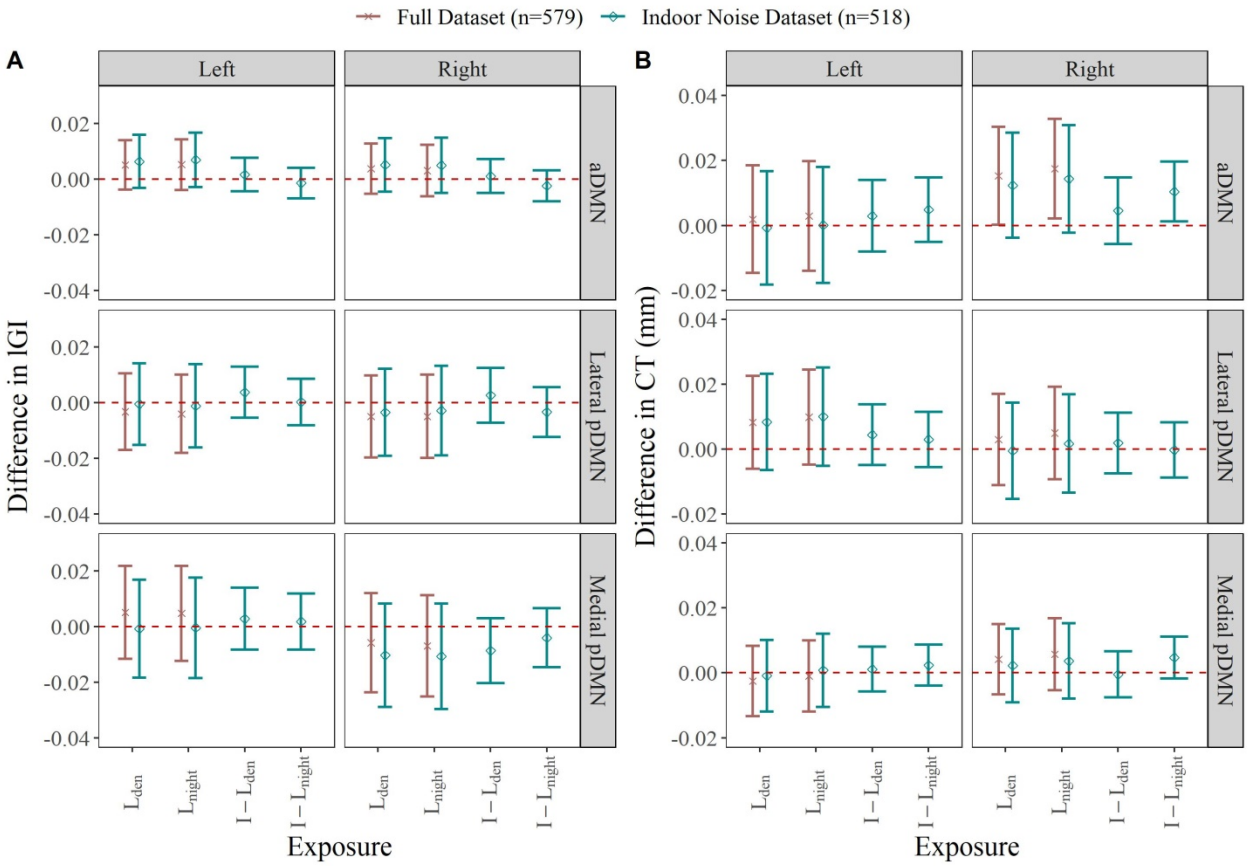

Fig. S4. Associations between outdoor and indoor noise, A) lGI, and B) cortical thickness (mm) within regions of the DMN in the right and left hemispheres of the brain. Estimates are shown for the full dataset (n=579) as well as the smaller dataset with complete indoor noise data (n=518). Associations were calculated per 10 dB(A) increase. Models were adjusted for age at MRI, sex, alcohol consumption, body mass index, diet, physical activity, smoking status, cumulative smoking, environmental tobacco smoke exposure, and $PM_{2.5abs}$.

Abbreviations: aDMN, anterior Default Mode Network; AP, air pollution; dB(A), A-weighted decibels; DMN, Default Mode Network; pDMN, posterior Default Mode Network; I-L_{den}, indoor 24-hour weighted noise; I-L_{night}, indoor nighttime noise; L_{den}, outdoor 24-hour weighted noise; lGI, local gyrification index; L_{night}, outdoor nighttime noise; $PM_{2.5abs}$, $PM_{2.5}$ absorbance

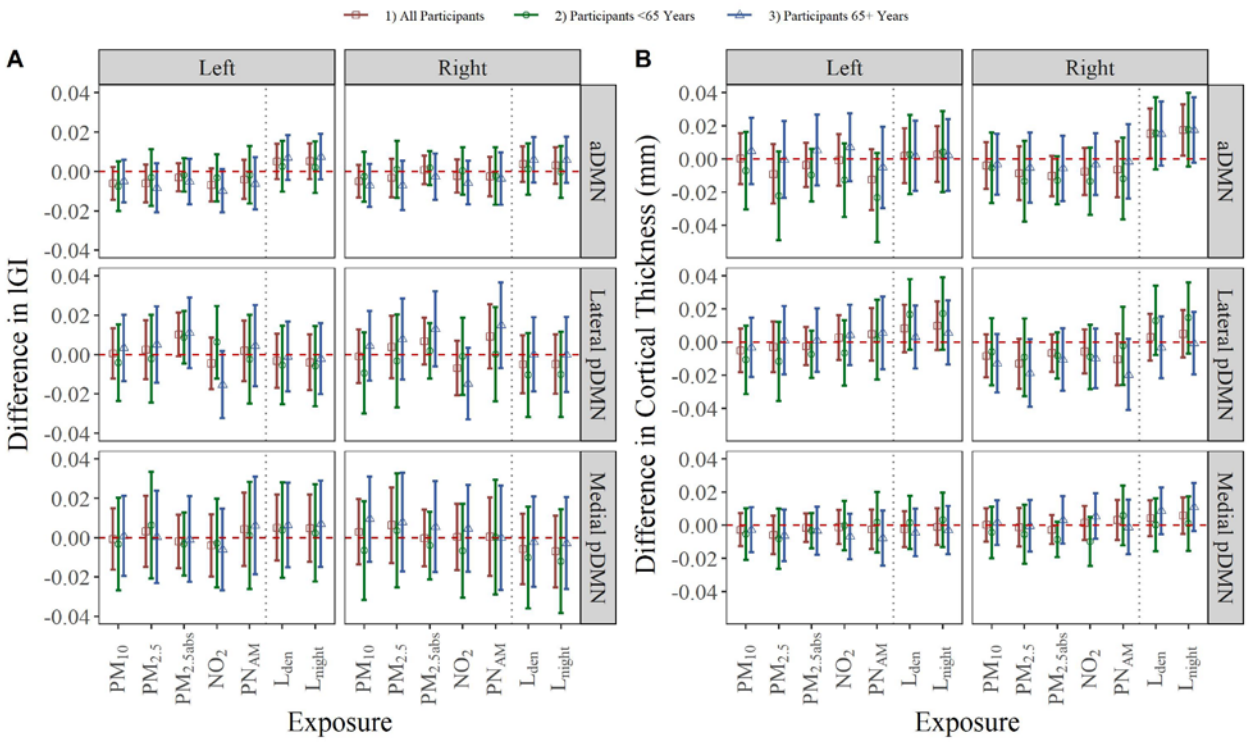

Fig. S5. Effect modification analyses evaluating associations between AP, noise, and A) lGI and B) cortical thickness in the DMN for all participants (n=579), among participants <65 years old at MRI (n=255), and among participants 65+ years old at MRI (n=324). Estimates for AP and noise were calculated per interquartile range or 10 dB(A) increase, respectively. All models adjusted for age, sex, body mass index, alcohol consumption, smoking status, cumulative smoking, environmental tobacco smoke exposure, diet, physical activity, and an interaction term between age category (<65 vs. 65+ years) and exposure. AP models were additionally adjusted for outdoor L_{den} whereas noise models were additionally adjusted for $PM_{2.5abs}$.

Abbreviations: aDMN, anterior Default Mode Network; AP, air pollution; dB(A), A-weighted decibels; DMN, Default Mode Network; lGI, local gyrification index; NO_2, nitrogen dioxide; L_{den}, outdoor 24-hour weighted noise; L_{night}, outdoor nighttime noise; pDMN, posterior Default Mode Network; PM_{10}, particulate matter with diameter ≤10 µm; $PM_{2.5}$, particulate matter with diameter ≤2.5 µm; $PM_{2.5abs}$, $PM_{2.5}$ absorbance; PN_{AM}, accumulation mode particle number concentration

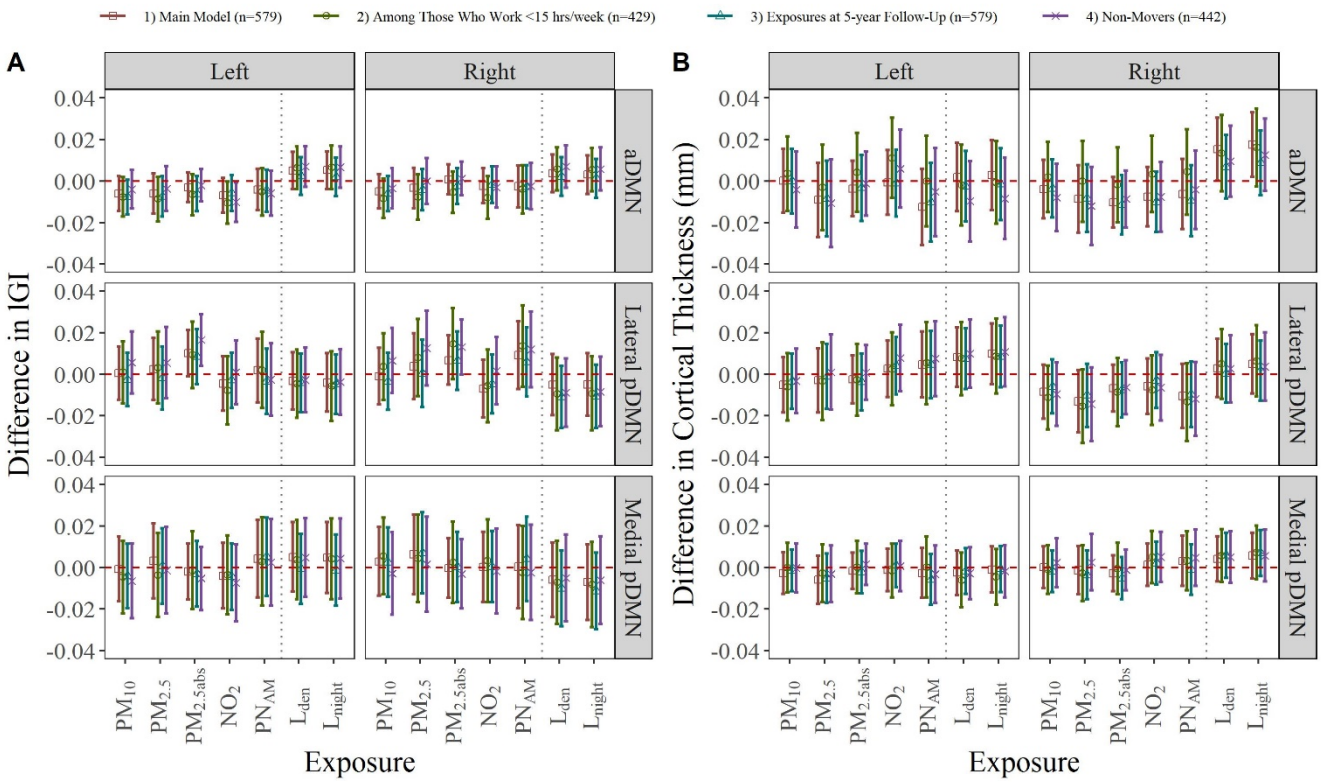

Fig. S6. Sensitivity analyses evaluating associations between AP, noise, and A) lGI and B) cortical thickness in the DMN among all participants (n=579), among participants who worked less than 15 hours per week at 10-year follow-up HNR examination (n=429), among all participants using exposures assigned at their 5-year HNR examination residential address (n=579), and among participants who did not move between HNR baseline and 1000BRAINS recruitment (n=442). All models adjusted for age, sex, body mass index, alcohol consumption, smoking status, cumulative smoking, environmental tobacco smoke exposure, diet, and physical activity. AP models were additionally adjusted for outdoor L_{den} whereas noise models were additionally adjusted for $PM_{2.5abs}$. Estimates for AP and noise were calculated per interquartile range or 10 dB(A) increase, respectively.

Abbreviations: aDMN, anterior Default Mode Network; AP, air pollution; dB(A), A-weighted decibels; DMN, Default Mode Network; HNR, Heinz Nixdorf Recall study; IQR, interquartile range; lGI, local gyrification index; NO_2, nitrogen dioxide; L_{den}, outdoor 24-hour weighted noise; L_{night}, outdoor nighttime noise; pDMN, posterior Default Mode Network; PM_{10}, particulate matter with diameter ≤10 µm; $PM_{2.5}$, particulate matter with diameter ≤2.5 µm; $PM_{2.5abs}$, $PM_{2.5}$ absorbance; PN_{AM}, accumulation mode particle number concentration